Hippocampus-lateral septum circuitry mediates foraging-related spatial memory in rats

Elizabeth A. Davis[1*], Clarissa M. Liu[1,2*], Isabella H. Gianatiempo[1], Andrea N. Suarez[1], Alyssa M. Cortella[1], Joel D. Hahn[3], and Scott E. Kanoski[1,2]

[*]These two authors contributed equally

[1]Human and Evolutionary Biology Section, Department of Biological Sciences, Dornsife College of Letters, Arts and Sciences, University of Southern California, 3616 Trousdale Pkwy, Los Angeles, CA, USA, 90089; [2]Neuroscience Graduate Program, University of Southern California, 3641Watt Way, Los Angeles, CA, USA. 90089; [3]Neurobiology Section, Department of Biological Sciences, Dornsife College of Letters, Arts and Sciences, University of Southern California, 3616 Trousdale Pkwy, Los Angeles, CA, USA, 90089

Corresponding author:
Scott E. Kanoski, PhD
University of Southern California
3616 Trousdale Parkway, AHF-252
Los Angeles, CA 90089-0372
Phone: 213-821-5762
Email: kanoski@usc.edu

Classification: Biological Sciences, Neuroscience

Keywords: feeding, cognition, place cells, motivation, reward, foraging, lateral hypothalamic area, prefrontal cortex

ABSTRACT

Remembering the location of a food or water source is essential for survival. Here we identify a hippocampal-septal neural circuit that is necessary for spatial memory based specifically on appetitive reinforcement. Both reversible and chronic disconnection of ventral hippocampus CA1 subregion (CA1v) projections to the lateral-septum (LS) using pathway-specific dual viral approaches impaired spatial memory retention for the location of either food or water reinforcement. However, disconnection of this pathway did not affect performance in an aversive escape-motivated spatial memory task that used the same apparatus and visuospatial cues. The selectivity of this pathway in mediating foraging-related spatial memory was further supported by results showing that CA1v-LS disconnection did not affect anxiety-like behavior, locomotor activity, or social and olfactory-based appetitive learning. To examine whether CA1v-LS mediation of foraging-related spatial memory involves collateral projections of CA1v neurons, we utilized virus-based neural pathway tracing analyses to identify the medial prefrontal cortex (mPFC) as a collateral target of LS-projecting CA1v neurons. However, functional disconnection of CA1v and mPFC did not affect appetitive spatial memory, thus further supporting the selectivity of CA1v-LS signaling for this behavior. The nucleus accumbens, lateral hypothalamic area, and other brain regions associated with food motivation and reward were identified as second-order targets of CA1v-LS signaling using a multisynaptic anterograde tracing approach. Collective results reveal that CA1v to LS communication plays a critical role in remembering an environmental location based on appetitive (food or water) but not aversive (escape) reinforcement, thus identifying a novel neural pathway regulating foraging-related memory processes.

INTRODUCTION

A survival advantage common to early humans and lower-order mammals is to accurately remember the location of a food or water source in the environment, and to then efficiently navigate back to a shelter or other safe location. The neurobiological substrates that regulate visuospatial navigation are therefore critical to effectively implement food-directed or water-directed foraging behavior. In rodents a number of maze tasks have been developed for studying spatial memory and navigation, including the widely popular Morris water maze that requires animals to swim and navigate to a submerged escape platform using distal viusospatial cues as a guide (1). The conceptually similar Barnes maze task requires animals to learn and recall a location for escaping mildly aversive stimuli (bright lights, loud noises) (2). These and other tasks have been instrumental in identifying brain structures within the telencephalon that are essential for visuospatial mapping and egocentric orientation in the environment, including the hippocampus and the medial entorhinal cortex, respectively (3, 4). However, despite that reliably locating food and water sources in the environment is a key selection pressure driving evolution of visuospatial navigation, the overwhelming majority of rodent model research on the substrates of spatial learning and memory have utilized procedures such as the Morris water maze and the Barnes maze that each involve escaping aversive reinforcement (5, 6). Furthermore, while single unit recordings have been used to identify specific populations of neurons that subserve distinct navigational functions (e.g., hippocampal “place cells”, medial entorhinal “grid cells”) (7, 8), the bulk of this research has recorded neural activity under neutral conditions void of either appetitive or aversive reinforcement. Very little research has been dedicated to identify brain regions and neural circuits that may specifically promote spatial memory based on the location of appetitive reinforcers (e.g., food, water), as well as the extent to which the nature of the reinforcement is a critical factor in deciphering the brain’s control of visuospatial navigation.

The majority of rodent model research investigating brain regions that mediate visuospatial navigational memory has focused on the anterior and “dorsal” subregion of the hippocampus (septal pole; HPCd). However, the posterior and “ventral” hippocampus subregion (temporal pole; HPCv), while classically associated with stress- and affect-associated memory processes (9), also plays a role in visuospatial learning and memory (10-12). For example, under

63 some testing conditions selective HPCv lesions impair spatial memory performance in the Morris
64 water maze (12, 13). Moreover, place cells that are responsive to changes in the visuospatial
65 environment are present within both the HPCd and HPCv pyramidal layers, with a linear
66 increase in the scale of representation from the dorsal to the ventral pole (11). Despite a common
67 role for the HPCd and HPCv in mediating spatial memory, there is also evidence for a functional
68 distinction between the subregions (9, 14, 15). For instance, lesions of the HPCv but not the
69 HPCd alter stress responses (16) and anxiety-like behavior (17), whereas HPCd but not HPCv
70 lesions impair spatial memory in an incidental (nonreinforced) procedure (18). These two HPC
71 subregions also have distinct afferent and efferent neural connections. This disparate
72 neuroanatomical connectivity supports a framework for a functional diversity in which the HPCd
73 preferentially processes cortical-derived sensory information and the HPCv preferentially
74 processes metabolic and limbic-derived affective information (9, 15). The functional distinction
75 between these two subregions is further supported by the generation of the hippocampus gene
76 expression atlas, which provides a comprehensive integration of gene expression and
77 connectivity across the HPC axis (19). Given that both the HPCv and the HPCd participate in
78 spatial memory but have distinct neuroanatomical connectivity and contributions when it comes
79 to regulating other cognitive and mnemonic processes, it is feasible that the HPCv and HPCd
80 support different forms of spatial memory depending on the type of reinforcement and/or the
81 context associated with the behavior.
82 Recent findings identify the HPCv as a critical brain substrate in regulating feeding
83 behavior and food-directed memory processes. Reversible inactivation of HPCv neurons after a
84 meal increases the size of and reduces the latency to consume a subsequent meal (20, 21). In
85 addition, receptors for feeding-related hormones are more abundantly expressed in the HPCv
86 compared to the HPCd (e.g., ghrelin receptors (22, 23), glucagon-like peptide-1 [GLP-1]
87 receptors (24)), and these HPCv endocrine and neuropeptide receptor systems alter food intake
88 and feeding-related memory (25). For example, leptin and GLP-1 act in the HPCv (CA1v
89 subregion) to decrease food intake and food-motivated conditioned behaviors (26-28), whereas
90 the orexigenic gut-derived hormone ghrelin administered to the HPCv but not HPCd has
91 opposite effects (25, 29). Olfactory information, which is intimately connected with feeding
92 behavior, is also preferentially processed within the HPCv compared with the HPCd. The CA1v,
93 specifically, is bidirectionally connected to brain regions that process olfactory information (9,

30, 31), and CA1v neurons respond more robustly to olfactory contextual cues compared with CA1d (10). Further, ghrelin signaling in the CA1v improves olfactory- and socially-mediated memory for food preference (32). Given the HPCv appetite-relevant neuroanatomical connections, endocrine and neuropeptide receptor expression profiles, and functional evidence linking this subregion with food-motivated behaviors, we hypothesize that HPCv mediation of visuospatial memory is preferentially biased to food and water-reinforced foraging behavior.

HPCv pyramidal neurons have extensive projection targets throughout the brain (33), yet the functional relevance of these pathways is poorly understood. Recently, CA1v projections to the medial prefrontal cortex (mPFC) and lateral hypothalamic area (LHA) were found to mediate feeding-related outcomes associated with GLP-1 and ghrelin signaling, respectively (28, 34). CA1v neurons also robustly target the LS (35, 36), and a HPCv dentate gyrus-CA3v to lateral septum (LS) pathway was identified that suppresses feeding (37). However, the relevance of this pathway to feeding-related learning and memory is unknown. It is feasible that CA1v to LS projections participate in regulating spatial memory for food location, a notion supported by findings showing that neuroplastic changes occur in the LS after learning a spatial memory task (38, 39). Thus, in addition to exploring the role of the HPCv in memory for the spatial location of food or water, the present study also investigated the specific role of the CA1v to LS pathway in foraging-relevant memory processes.

To systematically investigate the role of the HPCv and CA1v to LS signaling in visuospatial learning and memory for food and water reinforcement, we developed two novel appetitive reinforcement-based spatial foraging behavioral tasks that allows for direct comparison with an aversive reinforcement-based task of similar difficulty that uses the same apparatus and spatial cues. Performance in these tasks was assessed following pathway-specific dual viral-based reversible (chemogenetic inhibition) or chronic (targeted apoptosis) disconnection of the CA1v to LS pathway. To further expand neural network knowledge on CA1v to LS signaling, we used conditional viral-based neuroanatomical tracing strategies to identify both first-order collateral and second-order targets of LS-projecting CA1v neurons. Collective results from the present study identify novel neural circuitry of specific relevance to foraging behavior.

RESULTS

125

126 **The ventral hippocampus (HPCv) is required for remembering the spatial location of food**

127 To examine the importance of the HPCv in memory for the spatial location of food, animals
128 received bilateral *N*-Methyl-D-aspartate excitotoxic lesions of the HPCv (HPCv lesion n=12) or
129 bilateral sham injections (control n=12) (histological analyses for the neuron-specific NeuN
130 antigen in Fig. 1A) and were tested in a novel appetitive visuospatial memory task developed in
131 our lab. Results revealed no significant differences in errors (incorrect hole investigations) (Fig.
132 1E) or latency to locate the food source hole (Fig. 1F) during training. However, memory probe
133 results show that animals with HPCv lesions decreased the ratio of correct + adjacent / total holes
134 explored in the first minute compared with controls (Figure 1G; $p<0.05$, cohen's d=-1.0174).
135 Analysis for the combined 2-minute period did not yield a statistical difference between groups.
136 Post-surgical analyses of food intake (Supp. Fig. 1A) and body weight (Supp. Fig. 1B)
137 found no group differences in these measures over time. These collective results indicate the
138 HPCv is required for memory retention but not learning of the spatial location of food in the
139 environment.

140

141 **Ventral hippocampus CA1 (CA1v) projections to the lateral septum (LS) mediate**
142 **appetitive spatial memory for food and water location, but not aversive spatial memory for**
143 **escape location**

144 A major neuroanatomical target of HPCv CA1 neurons (CA1v) is the LS (36). We investigated
145 the functional relevance of the CA1v to LS signaling in learning and recalling the spatial location
146 of either food or water reinforcement using conditional dual viral approaches to either reversibly
147 (via cre-dependent pathway-specific inhibitory chemogenetics; diagram of approach in Fig. 2A)
148 or permanently (via cre-dependent pathway-specific caspase-induced lesions; diagram of
149 approach in Fig. 2B) disconnect CA1v to LS communication. Results from the appetitive food
150 seeking spatial memory task reveal no significant group differences during training in either
151 errors before locating the correct hole (Fig. 2E) or latency to locate the food source hole (Fig.
152 2F). However, memory probe results demonstrate that both acute (pathway-specific DREADDs)
153 and chronic (pathway-specific caspase) CA1v to LS disconnection decreased the ratio of correct
154 + adjacent / total holes explored in the entire two minutes of the probe compared with controls

155 (Fig. 2G; $p<0.05$, cohen's d=-1.142), with a similar trend in the first minute of the probe
156 ($p=0.059$).
157 Results from the appetitive water seeking spatial memory task in a separate cohort of rats
158 also reveal no significant group differences during training in either errors before locating the
159 correct hole (Fig. 2H) or latency to locate the food source hole (Fig. 2I). However, a significant
160 impairment following either acute or chronic CA1v to LS disconnection of ratio of correct +
161 adjacent / total holes explored in 2-min memory probe compared with controls (Fig 2J; $p<0.05$,
162 cohen's d=-1.18). Analysis for the first minute alone of the probe test did not yield a statistical
163 difference between groups.
164 Histological analyses confirmed successful viral transfection of LS-projecting CA1v
165 neurons with DREADDs (Figs. 2C&D) or caspase (Supp. Figs. 2E&F), and post-surgical
166 analyses of food intake (Supp. Fig 2A) and body weight (Supp. Fig 2B) found no group
167 differences in these measures over time (in the absence of CNO treatment). These data
168 demonstrate that CA1v to LS communication is critical for remembering the spatial location of
169 food and water, and that these effects are unlikely to be based on differences in energy status or
170 food motivation.
171 To evaluate whether the CA1v to LS pathway is specifically involved in appetitive
172 reinforcement-based spatial memory (food or water) vs. spatial memory in general, in a separate
173 cohort of animals we tested the effect of reversible and chronic CA1v to LS disconnection in a
174 spatial learning task based on aversive reinforcement rather than food. Importantly, this task uses
175 the same apparatus and visuospatial cues as the spatial location food and water memory tasks
176 described above, but the animals are motivated to locate the tunnel to escape mildly aversive
177 stimuli (bright lights, loud noise) with no food or water reinforcement in the tunnel (see Fig. 1B).
178 Training results revealed no significant group differences in errors before correct hole (Fig. 2K)
179 nor latency to locate the escape hole (Fig. 2L). During the memory probe test, there were no
180 group differences in the ratio of correct + adjacent / total holes investigated during the first
181 minute nor the entire two minutes (Fig. 2M) of the memory probe. Histological analyses
182 confirmed successful viral transfection of LS-projecting CA1v neurons with DREADDs (Figs.
183 2C&D) or caspase (Supp. Figs. 2E&F), and post-surgical analyses of food intake (Supp. Fig. 2C)
184 and body weight (Supp. Fig. 2D) found no group differences in these measures over time (in the
185 absence of CNO treatment). These collective findings suggest that CA1v to LS signaling

specifically mediates spatial memory in a reinforcement-dependent manner, playing a role in appetitive (food or water reward) but not aversive (escape-based) spatial memory.

Reversible, but not chronic disconnection of CA1v to LS signaling increases chow intake under free-feeding conditions.

While the results above suggest that the impairments in food or water-based spatial memory were not based on long-term changes in food intake or body weight, these experiments were conducted under conditions of either chronic food or water restriction. To examine the role of CA1v to LS signaling on feeding behavior under free-feeding conditions, we examined meal pattern feeding analyses in the caspase vs. the control group (chronic CA1v-LS disconnection), and in the DREADDs group following CNO or vehicle (within-subjects design; reversible CA1v-LS disconnection). Results averaged over 5d revealed no significant effect of chronic CA1v to LS disconnection (caspase group) on 24h meal frequency, meal size, meal duration, or 24h food intake in comparison to controls (Supp. Figs. 3A-D). However, acute and reversible silencing of LS-projecting CA1v neurons (DREADDs group; via lateral ventricular injection of the DREADD ligand CNO) significantly increased 24h chow intake (Supp. Fig. 3H; $p<0.05$, cohen's $d=0.10$) relative to vehicle treatment, accompanied by a trend towards increased meal frequency (Supp. Fig. 3E; $p=0.11$) and no effect on meal size or meal duration (Supp. Figs. 3F&G). These results are unlikely based on nonselective effects of the CNO, as we've recently shown that ICV CNO injections do not affect food intake in rats when tested under similar conditions (40). Collectively these findings show that reversible CA1v to LS disconnection increases food intake under free-feeding conditions, whereas food intake is not affected by chronic CA1v to LS ablation.

CA1v to LS disconnection does not affect nonspatial HPC-dependent appetitive memory

To examine the role of CA1v to LS signaling in a nonspatial HPC-dependent food-reinforced memory task, we tested the effect of reversible and chronic CA1v to LS disconnection in the social transmission of food preference (STFP) test (diagram in Fig. 3A). The HPCv plays an important role in STFP (32, 41, 42), which tests socially-mediated food-related memory based on previous exposure to socially-communicated olfactory cues. Results revealed that there were no differences in preference ratio between groups (Fig. 3B), with all three groups performing

217 significantly above chance (ps<0.05). These results suggest that neither acute nor chronic CA1v
218 to LS disconnection impair food-related memory based on social-based olfactory stimuli.
219
220 **CA1v to LS disconnection does not affect anxiety-like behavior or levels of locomotor**
221 **activity**
222 HPCv to LS circuitry has been shown to play a role in mediating anxiety and stress behavior (43-
223 45). Given that altered anxiety-like behavior and/or locomotion could produce behavioral
224 changes that may lead to an apparent spatial memory deficit in any of the spatial learning tasks
225 used, we examined whether HPCv to LS disconnection yields differences in anxiety-like
226 behavior (zero maze task; diagram of apparatus in Fig. 3C) and/or locomotion (open field test).
227 Results showed no significant group differences in time spent in the open zones in the zero maze
228 test (Fig. 3D) nor in the number of open zone entries (Fig. 3E), suggesting that neither chronic
229 nor reversible disconnection of the CA1v to LS circuitry influences anxiety-like behavior. In
230 addition, CA1v to LS disconnection had no effect on general locomotor activity in the open field
231 test (Fig. 3F). These results support that observed deficits in food-seeking and water-seeking
232 spatial memory are not secondary to general differences in anxiety-like behavior or locomotor
233 impairments in the disconnection groups.
234
235 **The medial prefrontal cortex is a collateral target of LS-projecting CA1v neurons**
236 In addition to the LS, CA1v neurons also robustly project to the medial prefrontal cortex
237 (mPFC) and the lateral hypothalamic area, two pathways that we have previously shown to be
238 involved in feeding behavior (27, 29, 34). To examine whether LS-projecting CA1v neurons
239 have collateral targets in the mPFC, LHA, or in other brain regions, we utilized a conditional
240 dual viral neural pathway tracing approach that identifies collateral targets of a specific
241 monosynaptic pathway (CA1v->LS; diagram of approach in Fig. 4A, representative CA1v
242 injection site in Fig. 4B, representative CA1v injection site in Fig. 4C). Results revealed that LS-
243 projecting CA1v neurons also project to the mPFC (Fig. 4D), whereas no labeling was observed
244 in the LHA, and very minimal labeling was observed in other brain regions. Thus, it may be the
245 case that the impaired spatial memory for food location observed following either reversible or
246 chronic CA1v to LS disconnection are based, in part, on CA1v to mPFC signaling from the same
247 CA1v to LS projecting neurons.

248

249 **Neither CA1v to mPFC nor CA1v to LHA signaling contribute to spatial memory for food**
250 **location**

251 We next sought to test the functional relevance to food-directed spatial memory of CA1v-
252 originating neural pathways that either do (CA1v to mPFC) or do not (CA1v to LHA)
253 collateralize from CA1 to LS projections. We also investigated the role of a pathway (CA1v to
254 LHA) that is not a target of LS-projecting CA1v neurons, but has previously been associated
255 with appetitive and consummatory aspects of feeding behavior (29, 34). Both the CA1v to mPFC
256 and CA1v to LHA projections are exclusively ipsilateral (27, 34), and thus these pathways allow
257 for a 'contralesional' approach to achieve chronic functional disconnection (diagram of approach
258 in Fig. 4E&4I, modified from (34)). This approach was utilized in favor of the dual viral
259 approaches used for the CA1v-LS disconnection as it does not require the use of viruses and
260 involves fewer surgical injections to achieve a similar goal. We note that this contralesional
261 approach is not a feasible option for the CA1v-LS pathway, as CA1v neurons project to the LS
262 bilaterally (e.g., Fig. 5F). Post-surgical analyses of food intake (Supp. Fig. 3A,C) and body
263 weight (Supp. Fig. 3B,D) found no group differences in these measures over time for either the
264 CA1v-mPFC or the CA1v-LHA disconnection groups. Training results from the appetitive
265 spatial memory task revealed no group differences in errors before locating the correct hole (Fig.
266 4F, 4J) or latency to locate the food-baited hole (Fig. 4G, 4K) for either the CA1v-mPFC or the
267 CA1v-LHA disconnection groups. Importantly, memory probe results demonstrate that neither
268 CA1v to mPFC nor CA1v to LHA disconnection altered the ratio of correct + adjacent / total
269 holes explored in the first minute or the entire two minutes (Fig. 4H, 4L) compared with
270 controls. These data collectively demonstrate that CA1v to LS mediation of foraging-related
271 memory does not require collateral projections to the mPFC neural pathway. Further, CA1v to
272 LHA neural signaling, which participates in other conditioned aspects of food intake (29, 34), is
273 not required for either learning or remembering of the spatial location of food.

274

275 **Second-order targets of CA1v to LS neurons include the mPFC, the LHA, and the ACB**

276 We used a dual viral tracing strategy (diagram of approach in Fig. 5A; representative LS
277 injection site in Fig. 5B) to identify downstream targets of LS-projecting CA1v neurons. Results
278 revealed that the mPFC (Fig. 5C), the LHA (Fig. 5D) and the nucleus accumbens (ACB; Fig. 5E)

are among the strongest second-order targets of the CA1v to LS-projecting neurons. Quantitative analyses using a custom-built data-entry platform (Axiome C, created by JDH) are summarized graphically for a representative animal on a brain flatmap summary diagram (Fig. 5F) for the hemisphere ipsilateral (top) and contralateral (bottom) to the injection sites. The data are also summarized in tabular form in Supplementary Table 1.

DISCUSSION

Memory for the physical location of a food or water source is adaptive for maintaining adequate energy supply for reproduction and survival. However, the neural circuits mediating this complex behavior are not well understood, as research on visuospatial memory has predominantly used tasks with either aversive or neutral/passive reinforcement. Moreover, whether the neural circuitry mediating spatial memory function is divergent based on the nature (e.g., appetitive vs. aversive) or modality (e.g., food vs. water) of the reinforcement has not been systematically investigated. The present study identified a monosynaptic CA1v to LS pathway as a necessary substrate for food- and water-motivated spatial memory. Moreover, the selectivity of the CA1v-LS pathway in mediating spatial memory for food and water location is supported by results showing that disconnection of this pathway did not affect performance in an escape-motivated spatial memory task of comparable difficulty conducted in the same apparatus, anxiety-like behavior, locomotor activity, or olfactory and social-based appetitive memory. Viral pathway tracing identified that LS-projecting CA1v neurons also send collateral projections to the mPFC, however, functional disconnection of CA1v-mPFC signaling did not impair spatial memory for food location. Utilization of an anterograde multisynaptic viral tracing approach and quantitative forebrain-wide axon mapping analyses revealed that the CA1v-LS pathway sends second-order projections to various feeding and reward-relevant neural substrates such as the LHA, ACB, and mPFC. Collectively, these data establish monosynaptic CA1v to LS signaling as essential for spatial memory-based foraging behavior, and we further identify a neural network of interconnected feeding-relevant substrates that are collateral and/or downstream targets of this pathway.

Historically, the hippocampus has been divided into the dorsal and ventral subregions that have both distinct and overlapping functions, anatomical connections, and genetic and receptor expression profiles (14, 15, 19, 33, 46). The HPCd has been predominantly implicated

310 in facilitating spatial memory, whereas the HPCv is linked with stress responses, affective
311 behavior, and energy balance. However, the HPCv also plays a role in spatial memory,
312 particularly for goal-directed navigation. Consistent with present results, a recent study found
313 that both the HPCd and HPCv were critical for food reward-directed spatial navigation in an
314 obstacle-rich complex environment (47). Under certain testing conditions, spatial learning and
315 memory in an aversive reinforcement-based water maze also requires both subregions of the
316 HPC (48). Similarly, whole-brain analysis of blood flow in rats during retrieval of spatial
317 memory in an aversive reinforcement-based Barnes maze task revealed increased activation in
318 the CA1d and CA1-3v in trained animals compared with controls (49). These results indicate that
319 spatial processing in the hippocampus is organized longitudinally, and that both HPCd and HPCv
320 are important for goal-directed spatial navigation. Here we expand this literature by identifying a
321 specific HPCv-originating pathway (CA1v->LS) that selectively mediates spatial memory for the
322 location of appetitive (food or water) reinforcement.
323 While HPCv neurons project widely throughout the neuraxis, projections to the LS are
324 particularly robust (36). The LS has been implicated in food anticipatory/seeking behavior,
325 where metabolic activation of the lateral septum peaks immediately before feeding (during food
326 anticipatory activity) in rabbit pups (50) and gamma-rhythmic input to the LHA from the LS
327 evokes food approach behavior (51). In addition, the LS can bidirectionally modulate food intake
328 via a number of feeding-relevant neuropeptides, including glucagon-like peptide-1, ghrelin, and
329 urocortin (52-54). A recent finding demonstrated that DREADDs-mediated disconnection of a
330 HPCv to LS pathway (from CA3v and DGv) increases food intake in mice, with
331 opposite/hyperphagic effects observed following activation of this pathway (37). Similarly, here
332 we demonstrate that DREADDs-mediated acute silencing of the CA1v to LS pathway increases
333 food intake in rats. Together these findings support a role for HPCv-LS signaling in regulating
334 feeding behavior. However, these results are based on analyses conducted in the home cage
335 where animals have free and unlimited access to food and water. Here we extend these findings
336 by examining the role of CA1v to LS signaling in foraging-relevant memory processes under
337 conditions that are more relevant to normal mammalian behavior, where food and water are not
338 freely available. Not only do our results identify a novel role for CA1v to LS signaling in
339 processing spatial memory for food and water reward location, but we further show that this

circuit appears to selectively promote spatial memory based on appetitive and not aversive-based reinforcement.

The use of two different but complementary approaches for neural pathway-specific disconnection allowed us to test at the levels of learning and memory separately. For example, the use of a reversible (DREADDs) disconnection procedure allowed us to evaluate the effect of CA1v to LS disconnection during the memory probe only, with circuit intact during training (CNO was not administered at any point during training). In contrast, the chronic (caspase) disconnection procedure was performed before training and therefore could have affected learning if CA1v to LS pathways were required for the learning of the task. However, our results showed that CA1v to LS did not impair learning, but rather, only memory retention performance in the probe test conducted days after the end of training. Thus, we can now confirm based on two complementary levels of analysis that this pathway is involved in longer-term memory recall but not learning/acquisition, which is consistent with recent evidence demonstrating that complete HPCv lesions impair retrieval (probe performance), but not acquisition (learning) in a Morris water maze (55).

Present results identify the CA1v-LS pathway in coordinating reward-motivated behavior with learned spatial information. While the use of aversive reinforcement-based spatial memory tasks are predominant, the radial arm maze has also been used to investigate food-motivated spatial memory (56). Specifically, the radial arm maze examines different components of spatial memory relevant to different foraging strategies. In win-shift tasks, animals learn to avoid previously visited reward arms, which models spontaneous alternation and exploration in environments with minimal resources. On the other hand, in win-stay tasks, animals learn to return to previously reinforced arms modeling foraging in environments of plentiful resources. An advantage of the present food-reinforced Barnes maze approach over the radial arm maze procedure is that we've developed parallel procedures that use the same apparatus and visuospatial cues to examine water- and escape-motivated spatial memory, thus offering a powerful approach to assess the selectivity of the circuit based on multiple reinforcement modalities (food vs. water vs. escape/aversive). While our results clearly support a role for the HPCv in food-reinforced spatial memory, a previous study utilizing a four-baited/four-unbaited version of the eight-arm radial maze task found that NMDA-mediated lesions of the HPCd, but not HPCv, impair spatial reference and working memory (57). Another study using a similar

371 procedure reported that complete HPC lesions impaired both spatial and working memory,
372 whereas lesions to either the HPCd, HPCv, or intermediate HPC had minimal effect on memory
373 performance (58). Future studies will needed to address whether discrepancies between the
374 present results and these studies are based on the differences between the behavioral tasks and/or
375 differences in loss of function methodologies. With regards to the latter, we note that our
376 pathway-specific chemogenetic and caspase-lesion approaches offered far greater specificity
377 (LS-projecting CA1v neurons vs. whole HPCv) compared with these studies.
378 Utilizing dual viral approaches and systematic forebrain-wide quantitative mapping
379 analyses, our findings confirm that the CA1v-LS pathway projects downstream to other neural
380 substrates involved in feeding and motivated behavior, including the LHA, ACB, and mPFC.
381 This experiment was performed to generate novel neural connectivity data for the field and to
382 demonstrate possible downstream 2nd-order targets that may inspire future research on these
383 newly-identified multi-order neural circuits. Given that metabolic activity in the LS and ACB is
384 associated with food anticipatory activity in rabbit pups (50), it is possible that the ACB is a
385 functional downstream target of CA1v-LS signaling for coordinating foraging behavior. It is less
386 likely, however, that the mPFC or the LHA are functional targets of CA1v-LS signaling for
387 appetitive spatial memory control based on the lack of effects on spatial memory for food
388 location when these pathways were disconnected. It is possible, however, that CA1v → LS →
389 mPFC (or → LHA) signaling is relevant to other mnemonic process, such as those involved in
390 drug-motivated or social-based memory tasks.
391 Collective results identify a CA1v to LS pathway involved in food- and water-motivated
392 spatial memory, but not escape-motivated spatial memory. Furthermore, the selectivity of this
393 pathway to appetitive spatial memory is supported by data showing that neither chronic nor
394 reversible disruption of CA1v to LS signaling influenced various other behavioral outcomes,
395 including anxiety-like behavior, locomotor activity, and nonspatial HPC-dependent appetitive
396 memory. We also systematically characterized collateral and second-order projections of this
397 pathway. Present results demonstrate overlapping pathways coordinated in the higher-order
398 control of energy balance, of which foraging behavior is an essential component, given that
399 foraging requires energy expenditure to locate food for subsequent energy intake. These data
400 shed light on the neural systems underlying complex learned and motivated behaviors that
401 require functional connections between cognitive and feeding-relevant substrates.

402

403 **METHODS**

404

405 **Animals**

406 Adult male Sprague–Dawley rats (Envigo; 250-275g on arrival) were individually housed
407 in hanging wire cages with *ad libitum* access (except where noted) to water and chow (LabDiet
408 5001, LabDiet, St. Louis, MO) on a 12h:12h reverse light/dark cycle. All procedures were
409 approved by the University of Southern California Institute of Animal Care and Use Committee.

410

411 **General intracranial injection procedures**

412 Rats were anesthetized via an intramuscular injection of an anesthesia cocktail (ketamine
413 90mg/kg body weight [BW], xylazine, 2.8mg/kg BW and acepromazine and 0.72mg/kg BW)
414 followed by a pre-operative, subcutaneous injection of analgesic (ketoprofen, 5mg/kg BW). Post-
415 operative analgesic (subcutaneous injection of ketoprofen, 5mg/kg BW) was administered once
416 per day for 3 days following surgery. The surgical site was shaved and prepped with iodine and
417 ethanol swabs, and animals were placed in a stereotaxic apparatus for stereotaxic injections.
418 NMDA or viruses were delivered using a microinfusion pump (Harvard Apparatus, Cambridge,
419 MA, USA) connected to a 33-gauge microsyringe injector attached to a PE20 catheter and
420 Hamilton syringe. Flow rate was calibrated and set to 83.3nl/sec. Injectors were left in place for
421 2min post-injection to allow for complete delivery of the infusate. Specific viruses/drugs,
422 coordinates, and injection volumes for procedures are detailed below. Following the completion
423 of all injections, incision sites were closed using either surgical staples, or in the case of
424 subsequent placement of an indwelling cannula, simple interrupted sutures. Upon recovery from
425 anesthesia and return to dorsal recumbency, animals were returned to the home cage. All
426 behavioral procedures occurred 21 days after injections to allow for complete transduction and
427 expression of the viruses, or complete lesioning drugs. General intracranial injection procedures
428 were followed for all injection procedures below.

429

430 **Chronic lesions of the HPCv**

431 Lesion animals received bilateral excitotoxic HPCv lesions via intracranial injections of
432 N-methyl-d-aspartate (NMDA; 4ug in 200nL; 100uL per hemisphere) at the following

433 coordinates at three different sites along the rostrocaudal extent of the HPCv (59): [1] -4.8mm
434 AP, +/-5.0mm ML, -7.5mm DV, [2] -5.5mm AP, +/-4.5mm ML, -7.0mm DV, and [3] -6.1mm
435 AP, +/-4.8mm ML, -7.0mm DV with control animals receiving vehicle saline in the same
436 location. The reference points for AP and ML coordinates were defined at bregma, and the
437 reference point for the DV coordinate was defined at the skull surface at the target site.
438 Bilateral HPCv lesion brains were histologically evaluated for the correct placement of
439 lesions in 1 out of 5 series of brain tissue sections. Neurons were visualized using
440 immunohistochemistry for the neuron specific antigen NeuN (see Immunohistochemistry). The
441 extent of NMDA lesions was determined postmortem by immunohistochemical detection of the
442 neuronal marker NeuN. Rats showing pronounced (~65%) loss of NeuN labeling within the
443 target region compared with the representative NeuN expression following sham injections in the
444 control group (average HPCv count of NeuN+ cells in control group) were included in data
445 analysis (34). Representative images in Fig. 1A.
446
447 **Acute and chronic disconnection of the CA1v to LS neural pathway**
448 Cre-dependent dual viral strategies were used to generate the following groups: [1] acute
449 chemogenetic disconnection of the CA1v to LS neural pathway (DREADDs; diagram of
450 approach in Fig. 2A), [2] chronic disconnection of the CA1v to LS neural pathway (caspase
451 lesion-induced; diagram of approach in Fig. 2B), and [3] a common/shared control group for
452 these two disconnection strategies. Regardless of group, all animals received a bilateral AAV
453 retro-cre injection in the LS (AAV2[retro]-hSYN1-EGFP-2A- iCre-WPRE; 200nL per side) at
454 the following stereotaxic coordinates (59): +0.84mm AP, +/-0.5mm ML, −4.8mm DV, all
455 defined at bregma.
456 According to experimental group, animals received a different virus delivered to the
457 CA1v subregion of the HPCv. All viruses were administered to the CA1v at the following
458 stereotaxic coordinates (59): −4.9mm AP defined at bregma, +/-4.8mm ML defined at bregma,
459 −7.8mm DV defined at skull surface at target site.
460 *[1] DREADDs group for reversible inactivation of CA1v to LS:* To allow reversible
461 chemogenetic inactivation of the CA1v to LS neural pathway, one group of animals received a
462 bilateral CA1v injection of a cre-dependent virus to drive expression of inhibitory designer
463 receptors activated by designer drugs (DREADDs), (AAV-Flex-hm4Di-tdTomato). This dual

464 viral strategy drives expression of inhibitory DREADDs exclusively in LS-projecting CA1v
465 neurons, which enables acute inactivation of these neurons by injection of the DREADDs ligand,
466 clozapine-N-oxide (CNO), at the time of behavioral testing.
467 *[2] Caspase group for chronic inactivation of CA1v to LS:* To allow chronic
468 disconnection of the CA1v to LS neural pathway, a second group of animals received a bilateral
469 CA1v cre-dependent caspase virus (AAV1-Flex-taCasp3-TEVp; 200nL per side) mixed with a
470 cre-dependent reporter virus (AAV-flex-tdTomato; 200nL per side) for histological verification.
471 This dual viral strategy drives expression of the apoptosis-mediator molecule caspase exclusively
472 in LS-projecting CA1v neurons, which induces apoptotic cell death in these neurons while
473 leaving other CA1v neurons intact.
474 *[3] Common control:* A common control group was generated so that the DREADDs and
475 caspase groups could both be compared to the same control group, instead of two different
476 control groups for the DREADDs and caspase groups, respectively. This allowed us to reduce
477 the number of animals needed for the same experimental objective. Thus, all animals received an
478 indwelling cannula and ICV injections of CNO as described below.
479 Immediately following viral injections, all animals were surgically implanted with a
480 unilateral indwelling intracerebroventricular (ICV) cannula (26-gauge, Plastics One, Roanoke,
481 VA) targeting the lateral ventricle (VL). Cannulae were implanted and affixed to the skull with
482 jeweler's screws and dental cement at the following stereotaxic coordinates: −0.9mm AP defined
483 at bregma, +1.8mm ML defined at bregma, −2.6mm DV defined at skull surface at site.
484 Placement for the VL cannula was verified by elevation of blood glucose resulting from an
485 injection of 210µg (2µL) of 5-thio-D-glucose (5TG) using an injector that extended 2mm beyond
486 the end of the guide cannula (60). A post-injection elevation of at least 100% of baseline
487 glycemia was required for subject inclusion. Animals that did not pass the 5TG test were retested
488 with an injector that extended 2.5mm beyond the end of the guide cannula and, upon passing the
489 5TG test, were subsequently injected using a 2.5mm injector instead of a 2mm injector for the
490 remainder of the study. Prior to behavioral testing where noted, all animals received an ICV
491 18mmol infusion (2uL total volume) of the DREADDs ligand clozapine N-oxide (CNO) (61),
492 rendering only DREADDs animals chemogenetically inactivated. CNO injections were hand
493 delivered using a 33-gauge microsyringe injector attached to a PE20 catheter and Hamilton

494 syringe through the indwelling guide cannulae. Injectors were left in place for 30sec to allow for
495 complete delivery of the CNO.
496 Cre-dependent DREADD expression targeting LS-projecting neurons in CA1v was
497 evaluated based on localization of the fluorescent reporter tdTomato. Immunohistochemistry for
498 red fluorescent protein (RFP) was conducted to amplify the tdTomato signal (see
499 Immunohistochemistry). Only animals with tdTomato expression restricted within CA1v neurons
500 were included in subsequent behavioral analyses. Representative images in Figs. 2C&D.
501 The general approach for neuronal apoptosis due to activation of cre-dependent caspase
502 targeting LS-projecting neurons in CA1v was validated in a separate cohort (n=8) based on
503 reduction of a cre-dependent fluorescent reporter tdTomato due to neuron cell death compared
504 with controls. The caspase group brains (which received a retro-cre virus in the LS in
505 conjunction with an injection of cre-dependent caspase virus mixed with a cre-dependent virus
506 that drives a tdTomato fluorescent reporter in the CA1v) were compared to control brains (that
507 received a retro-cre virus in the LS in conjunction with only a cre-dependent that drives a
508 tdTomato fluorescent reporter in the CA1v, which was equivalently diluted to match the caspase
509 injections). In both groups, immunohistochemistry for red fluorescent protein (RFP) was
510 conducted to amplify the tdTomato signal (see Immunohistochemistry). Confirmation of
511 successful caspase-driven lesions in the CA1v using this approach was evaluated by reduced
512 tdTomato fluorescence in comparison to control animals, with the expression of CA1v tdTomato
513 expression in the caspase group less than 15% of that observed in controls, on average
514 (Representative images in Supplementary Figs 2E&F). While this cohort allowed for successful
515 validation of the pathway-specific disconnection caspase approach, to improve the viability of
516 the animals for long-term behavioral analyses, the 3rd AAV with the fluorescent reporter (cre-
517 dependent tdTomato AAV) was omitted for cohorts undergoing behavioral analyses. For these
518 groups, histological confirmation for inclusion in subsequent statistical analyses was based on
519 identification of injections sites confined with the LS and CA1v, as observed using darkfield
520 microscopy.
521
522
523 **Identification of collateral targets of CA1v to LS projecting neurons**

524 Collateral targets of the CA1v to LS neural pathway were identified using a dual viral
525 approach (diagram of approach in Fig. 4A) where a retrograde vector was injected into the LS
526 (AAV2retro-hSyn1-eGFP-2A-iCre-WPRE; 200nL per side; coordinates as above), and a Cre-
527 dependent anterograde vector (AAV1-CAG-Flex-tdTomato-WPRE-bGH; 200nL per side;
528 coordinates as above) was injected in the CA1v. This latter injection drives tdTomato transgene
529 expression in CA1v neurons that project to the LS, which allows for brain-wide analyses of
530 collateral targets. After 3 weeks of incubation time to allow for complete transduction and
531 expression of the viruses, brains were collected, immunohistochemically processed, and imaged
532 as described below.
533
534 **Contralesional disconnection of the CA1v to mPFC neural pathway or the CA1v to LHA**
535 **neural pathway**
536 To functionally disconnect the CA1v to mPFC pathway (diagram of approach in Fig. 4E),
537 or the CA1v to LHA pathway (diagram of approach in Fig. 4J) lesion animals received a
538 unilateral excitotoxic CA1v lesion via an intracranial injection of NMDA (200nL) at the
539 following coordinates (36): −4.9mm AP defined at bregma, + or - 4.8mm ML defined at bregma
540 (left/right counterbalanced to be contralateral to mPFC or LHA lesion within-animal), −7.8mm
541 DV defined at skull surface at site, with control animals receiving vehicle saline injections in the
542 same location.
543 In addition to the CA1v lesion, CA1v to mPFC disconnect animals also received a
544 unilateral excitotoxic mPFC lesion via two intracranial injections of NMDA (4ug in 200nL;
545 100nL per injection) at the following coordinates (59): [1] +2.7mm AP, + or - 0.7mm ML
546 (left/right counterbalanced to be contralateral to CA1v lesion within-animal), −5.3mm DV and
547 [2] +3.0mm AP, + or - 0.7mm ML (left/right counterbalanced to be contralateral to CA1v lesion
548 within-animal), −4.7mm DV, with control animals receiving vehicle saline in the same location.
549 The reference points for all mPFC coordinates were defined at bregma.
550 In addition to the CA1v lesion, CA1v to LHA disconnect animals also received a
551 unilateral excitotoxic LHA lesion via an intracranial injection of NMDA (100nL per injection) at
552 the following coordinates (59): +2.9mm AP, + or – 1.1mm ML (counterbalanced to be
553 contralateral to CA1v lesion within-animal), −8.9mm DV, with control animals receiving vehicle

554 saline in the same location. The reference points for all LHA coordinates were defined at
555 bregma.
556 Contralesional brains were histologically evaluated for the correct placement of lesions by
557 visualizing neurons using immunohistochemistry for the neuron specific antigen NeuN (see
558 Immunohistochemistry). The extent of NMDA lesions was determined postmortem by
559 immunohistochemical detection of the neuronal marker NeuN. Rats showing pronounced (65%)
560 loss of NeuN labeling within the target region compared with a sham injection in the
561 contralateral side were included in data analysis (34).
562
563 **Identification of second order targets of CA1v to LS projecting neurons**
564 To identify second order targets of CA1v to LS-projecting neurons (diagram of approach
565 in Fig. 5A), animals received a bilateral injection of a transsynaptic Cre-inducing anterograde
566 vector into CA1v (AAV1-hSyn-Cre-WPRE-hGH; 200nL per side; coordinates as above) that
567 drives expression of Cre in both first-order (CA1v injection site) and 2nd-order (but not 3rd-
568 order) neurons via transsynaptic virion release (62, 63). This was combined with a bilateral
569 injection of a Cre-dependent anterograde vector in the LS (AAV1-CAG-Flex-tdTomato-WPRE-
570 bGH; 200nL per side, coordinates as above). This latter injection allows for anterograde tracing
571 from 1st-order LS targets receiving synaptic input from CA1v. After 3 weeks of incubation time
572 to allow for complete transduction and expression of the viruses, brains were collected,
573 immunohistochemically processed, and imaged as described below.
574 Data were entered using a custom built data-entry platform (Axiome C, created by JDH)
575 built around Microsoft Excel software and designed to facilitate entry of data points for all gray
576 matter regions across their atlas levels as described in a rat brain reference atlas: Brain Maps 4.0
577 (59). The Axiome C approach was used previously to facilitate the analysis of brain gene-
578 expression data (64). An ordinal scale, ranging from 0 (absent) to 7 (very strong), was used to
579 record the qualitative weight of anterograde labeling. An average value was then obtained for
580 each region across its atlas levels for which data were available. These data are summarized
581 graphically for a representative animal on a brain flatmap summary diagram (adapted from (65)).
582
583 **Food intake and body weight**

584 For the day prior to surgery (day 0) and for two weeks thereafter, 24h chow intake was
585 measured daily just prior to dark cycle onset to determine effects of experimental procedures on
586 food intake. Spillage was accounted for daily by collecting crumbs onto Techboard paper placed
587 under the cages of each animal. Additionally, animals were weighed daily just prior to dark cycle
588 onset to determine effects of experimental procedures on body weight.
589
590 **Meal pattern**
591 Meal size, meal frequency, meal duration, and cumulative 24h food intake were
592 measured using Biodaq automated food intake monitors (Research Diets, New Brunswick, NJ).
593 Rats (control n=7, caspase n=8, and DREADDs n=8) were acclimated to the Biodaq on ad
594 libitum chow for 3 days. Caspase group vs. control group feeding behavior data were collected
595 over a 5-day period (untreated, between-subjects design). The DREADDs group was tested using
596 a 2-treatment within-subjects design. Rats received 18mmol infusion of ICV CNO (2uL total
597 volume) or vehicle (daCSF, 33% dimethyl sulfoxide in artificial cerebrospinal fluid) 1h prior to
598 lights off and 24h feeding behavior was measured. Meal parameters were set at minimum meal
599 size=0.2g and maximum intermeal interval=600s.
600
601 **Appetitive food seeking spatial memory task**
602 To test visuospatial learning and memory for food reinforcement, we developed a novel
603 spatial food seeking task modified from the traditional Barnes maze procedure (6). Throughout
604 this paradigm, animals were maintained at 85% free-feeding body weight. The procedure
605 involves an elevated gray circular platform (diameter: 122cm, height: 140cm) consisting of 18
606 uniform holes (9.5cm diameter) spaced every twenty degrees around the outside edge. Under one
607 of the holes is a hidden tunnel (38.73cm L x 11.43cm W x 7.62cm D and a 5.08cm step).
608 Surrounding the table are distinct spatial cues on the wall (e.g. holiday lights, colorful shapes,
609 stuffed unicorn) that are readily visible to the animal. In contrast to the traditional Barnes Maze
610 where an animal uses the spatial cues to escape mildly aversive stimuli in the environment (e.g.
611 bright light and loud sound), this task utilizes food as motivation, such that each hidden tunnel
612 contained five 45mg sucrose pellets (Bio-Serv, Flemington, NJ). Additionally, a quiet white
613 noise (60dB) was used to drown out background noise and floor lamps were used for low-level
614 ambient lighting. On the first day, each animal underwent a habituation session consisting of

615 1min inside a transport bin under the table, 2min underneath the start box in the center of the
616 table, and 3min inside the hidden tunnel with 5 sucrose pellets. During training, each rat was
617 assigned a specific escape hole according to the position of the spatial cues with the location
618 counterbalanced across groups. Before each trial, animals were placed in the start box for 30
619 seconds. Animals were trained over the course of two 5-min trials per day for four days (five
620 days in contralesional experiments) to learn to use the spatial cues in order to locate the correct
621 hole with the hidden tunnel with sucrose pellets. After finding the correct hole and entering the
622 hidden tunnel during each 5min training session, animals were allowed to remain in the hidden
623 tunnel for 1 minute, and consistently consumed all 5 sucrose pellets at this time. In the event that
624 a rat did not find the correct hole during the 5min training session, the experimenter gently
625 guided the rat to the correct hole and were allowed to crawl in and then complete the training in
626 the same fashion as rats that found the hole on their own. Learning during training was scored
627 via animal head location tracking by AnyMaze Behavior Tracking Software (Stoelting Co.,
628 Wood Dale, IL). The incorrect hole investigations prior to finding the correct hole with sucrose
629 pellets ("errors before correct hole") as well as time to finding the correct hole ("latency to
630 correct hole") were calculated as an average of the two trials per day, and examined across days
631 of training.
632 After the conclusion of training, rats had a two-day break where no procedures occurred,
633 then were tested in a single 2min memory probe in which the hidden tunnel and sucrose pellets
634 were been removed. All animals received an ICV 18mmol infusion of CNO (2uL total volume)
635 1h prior to the memory probe, rendering only DREADDs animals chemogenetically inactivated
636 by CNO. In the memory probe, the ratio of the correct hole plus adjacent hole investigations over
637 the total number of hole investigations were calculated via animal head location tracking by
638 AnyMaze Behavior Tracking Software (Stoelting, Wood Dale, IL). This dependent variable was
639 selected a priori instead of correct hole only investigations based on recent findings
640 demonstrating that taste-responsive hippocampal neurons exhibit weaker spatial selectivity in
641 comparison to non-taste-responsive hippocampal neurons (66). When establishing and refining
642 the food-reinforced spatial memory procedure in multiple cohorts of rats, our preliminary data
643 revealed that memory probe effects in normal/control animals are either stronger in the 1st
644 minute, or in the 1st two minutes combined (but not the 2nd minute alone), with some cohorts
645 showing larger paradigm effects in minute 1, and others in minutes 1+2. Thus, for all

646 experiments presented we analyzed both the 1st minute and the 1st two minutes combined based
647 on an a priori determination from our preliminary studies. A diagram of the apparatus used for
648 the spatial foraging task is included in Fig. 1B.
649 During training sucrose pellets were taped underneath all of the holes to preclude
650 olfactory-based search strategies during training. Importantly, the memory probe test does not
651 include any sucrose pellets in the apparatus at all, and therefore there is no possibility of sucrose
652 odor cues to influence memory probe performance.
653
654 **Appetitive water seeking spatial memory task**
655 We modified our spatial food seeking task to utilize water reward instead of food reward.
656 Throughout this paradigm, animals were water restricted and received 90-min access to water
657 daily (given at least 1hr after the termination of behavioral procedures each day). In addition to
658 the habituation parameters described above, animals in this task were subjected to two 10-min
659 habituation sessions in the hidden tunnel with a full water dish prior to training, which allowed
660 them to become accustomed to reliably drinking from the water dish in the hidden tunnel.
661 Training procedures were the same as for the food-based task above, except instead of sucrose
662 pellets in the hidden tunnel, a water dish containing ~100 mL of water was placed in the back of
663 the hidden tunnel during training, and animals were allowed to remain in the hidden tunnel for
664 2min (instead of 1min, as above). Each animal consumed a minimum of 2mL of water during
665 this time for the training sessions. This newly-developed procedure allowed us to test spatial
666 learning and memory motivated by water reward using similar apparatus and stimulus conditions
667 to the food-reinforced task.
668
669 **Aversive spatial memory escape task (Barnes maze)**
670 To test visuospatial learning and memory for escape reinforcement, we used a modified
671 traditional Barnes maze procedure, which is a visuospatial-based escape task (6). Procedures
672 were exactly the same as above (appetitive spatial memory food seeking and water seeking tasks,
673 using the same apparatus, in the same room, and with the same visuospatial cues) aside from the
674 omission of the sucrose pellets or water dish in the hidden tunnel, the presence of mildly aversive
675 bright (120W) overhead lighting instead of dim ambient lighting, and a mildly aversive loud
676 white noise (75dB) instead of a quiet white noise (60dB). This allowed us to test spatial learning

677 and memory motivated by escape from aversive stimuli in a nearly-identical procedure to our
678 spatial foraging test for learning and memory motivated by palatable food or water consumption.
679 A diagram of the apparatus used for the spatial escape task is included in Fig. 1B.
680
681 **Social transmission of food preference (STFP)**
682 To examine food-related memory based on social- and olfactory-based cues, we utilized
683 the social transmission of food preference (STFP) task and adapted protocols from (32, 42, 67,
684 68). Briefly, untreated normal adult rats are designated as 'Demonstrators', while experimental
685 groups are designated as 'Observers'. Demonstrators and Observers are habituated to a powdered
686 rodent chow [LabDiet 5001 (ground pellets), LabDiet, St. Louis, MO] overnight. 24h later,
687 Observers are individually paired with demonstrators and habituated to social interaction, where
688 rat pairs are placed in a social interaction arena (23.5cm W × 44.45cm L × 27cm H clear plastic
689 bin with Sani-chip bedding) and allowed to interact for 30min. Both Observers and
690 Demonstrators are returned to their home cages and food is withheld for 23hr prior to the social
691 interaction. For the social interaction, Demonstrators are given the opportunity to consume one
692 of two flavors of powdered chow (flavored with 2% marjoram or 0.5% thyme; counterbalanced
693 according to group assignments) for 30min in a room separate from Observers. Our pilot studies
694 and previous published work (68, 69) show that rats equally prefer these flavors of chow. The
695 Demonstrator rat is then placed in the social interaction arena with the Observer rat, and the pairs
696 are allowed to socially interact for 30min. Observers are then returned to their home cage and
697 allowed to eat *ad libitum* for 1h and then food is removed. The following day, the 23h food-
698 deprived Observer animals are given a home cage food preference test for either the flavor of
699 chow paired with the Demonstrator animal, or a novel, unpaired flavor of chow that is a flavor
700 that was not given to the Demonstrator animal (2% marjoram vs. 0.5% thyme; counterbalanced
701 according to group assignments). All animals received an ICV 18mmol infusion of CNO (2uL
702 total volume) 1h prior to the social interaction session, rendering only DREADDs animals
703 chemogenetically inactivated by CNO. Food intake (1h) was recorded with spillage accounted
704 for by collecting crumbs onto Techboard paper that is placed under the cages of each animal.
705 The % preference for the paired flavor is calculated as: 100*Demonstrator-paired flavored chow
706 intake/Demonstrator + Novel flavored chow intake. In this procedure, normal untreated animals

707 learn to prefer the Demonstrator paired flavor based on social interaction and smelling the breath
708 of the Demonstrator rat (32, 42, 67-69). A diagram of the STFP procedure is included in Fig. 3E.
709
710 **Zero maze**
711 The zero maze behavioral paradigm was used to evaluate anxiety-like behavior. The zero
712 maze apparatus used was an elevated circular track, divided into four equal length sections. Two
713 zones were open with 3 cm high curbs ('open zones'), whereas the two other zones were closed
714 with 17.5 cm high walls ('closed zones'). All animals received an ICV 18mmol infusion of CNO
715 (2uL total volume) 1h prior to testing, rendering only DREADDs animals chemogenetically
716 inactivated by CNO. Behavioral testing was performed during the light cycle. Animals were
717 placed in the maze for a single, 5min trial in which the location of the center of the animal's
718 body was measured by AnyMaze Behavior Tracking Software (Stoelting, Wood Dale, IL). The
719 apparatus was cleaned with 10% ethanol in between animals. During the trial, the number of
720 open zone entries and total time spent in open sections (defined as body center in open sections)
721 were measured, which are each indicators of anxiety-like behavior in this procedure. A diagram
722 of the zero maze apparatus is included in Fig. 3G.
723
724 **Open field**
725 An open field test was used to evaluate general levels of locomotor activity. The
726 apparatus used for the open field test was an opaque gray plastic bin (60cm × 56cm), which was
727 positioned on a flat table in an isolated room with a camera directly above the center of the
728 apparatus. Desk lamps were positioned to provide indirect lighting to all corners of the maze
729 such that the lighting in the box uniformly measured 30 lux throughout. All animals received an
730 ICV 18mmol infusion of CNO (2uL total volume) 1h prior to testing rendering only DREADDs
731 animals chemogenetically inactivated by CNO. Behavioral testing began at dark onset. At the
732 start of the 10min test, each animal was placed in the open field apparatus in the same corner
733 facing the center of the maze. The location of the center of the animal's body was measured with
734 the AnyMaze Behavior Tracking Software (Stoelting, Wood Dale, IL). Total distance traveled
735 was measured by tracking movement from the center of the animal's body throughout the test.
736
737 **Immunohistochemistry**

738 Rats were anesthetized via an intramuscular injection of an anesthesia cocktail (ketamine
739 90mg/kg BW xylazine, 2.8mg/kg BW and acepromazine and 0.72mg/kg BW) then transcardially
740 perfused with 0.9% sterile saline (pH 7.4) followed by 4% paraformaldehyde (PFA) in 0.1M
741 borate buffer (pH 9.5; PFA). Brains were dissected from the skull and post-fixed in PFA with
742 15% sucrose for 24h, then flash frozen in isopentane cooled in dry ice. Brains were sectioned to
743 30µm thickness on a freezing microtome. Sections were collected in 5-series and stored in
744 antifreeze solution at −20°C until further processing. General fluorescence IHC labeling
745 procedures were performed as follows. The antibodies and dilutions that were used are as
746 follows: [1] For lesion histology using the neuron-specific protein NeuN, the rabbit anti-NeuN
747 primary antibody (1:1000, Abcam) was used followed by a donkey anti-rabbit conjugated to
748 AF488 (1:500, Jackson Immunoresearch). [2] To amplify the native tdTomato signal for
749 neuroanatomical tracing or DREADDs histology, the rabbit anti-RFP primary antibody (1:2000,
750 Rockland) was used followed by a donkey anti-rabbit conjugated to Cy3 (1:500, Jackson
751 Immunoresearch). [3] To amplify the native GFP signal for LS injection site histology, the
752 chicken anti-GFP primary antibody (1:500, Abcam) was used followed by a donkey anti-chicken
753 secondary antibody conjugated to AF488 (1:500, Jackson Immunoresearch). Antibodies were
754 prepared in 0.02M potassium phosphate buffered saline (KPBS) solution containing 0.2% bovine
755 serum albumin and 0.3% Triton X-100 at 4°C overnight. After thorough washing with 0.02M
756 KPBS, sections were incubated in secondary antibody solution. All secondary antibodies were
757 obtained from Jackson Immunoresearch and used at 1:500 dilution at 4°C, with overnight
758 incubations (Jackson Immunoresearch; West Grove, PA, USA). Sections were mounted and
759 coverslipped using 50% glycerol in 0.02 M KPBS and the edges were sealed with clear nail
760 polish. Photomicrographs were acquired using a Nikon 80i (Nikon DSQI1,1280X1024
761 resolution, 1.45 megapixel) under epifluorescence or darkfield illumination.
762 Lesions and virus expression were quantified in one out of five series of brain tissue sections and
763 analyses were performed in sections from Swanson Brain Atlas level 34-36 (59). The inclusion /
764 exclusion criteria are described above in the methods of each of these experiments.
765
766 **Statistics**
767 Data are expressed as mean +/- SEM. Differences were considered to be statistically
768 significant at $p<0.05$. All variables were analyzed using the advanced analytics software package

Statistica (StatSoft, Tulsa, OK, USA). For all measures of food intake, body weight, and errors/latency during spatial foraging and spatial escape task training, differences between groups were evaluated using two-way repeated measures ANOVAs (treatment x time). For lesion experiments, measures during spatial foraging and spatial escape task probes, differences between groups were evaluated using two-tailed independent two-sample Student's t-tests. For CA1v to LS disconnection experiments, measures during spatial foraging and spatial escape task probes, the STFP paradigm, the zero maze paradigm, and the open field test, differences between groups were evaluated using one-way ANOVAs. Significant ANOVAs were analyzed with a Fisher's LSD posthoc test where appropriate. Outliers were identified as being more extreme than the median +/- 1.5 * interquartile range. For all experiments, assumptions of normality, homogeneity of variance (HOV), and independence were met where required.

CONFLICT OF INTEREST

No conflicts of interest.

ACKNOWLEDGEMENTS

This work was supported by National Institute of Diabetes and Digestive and Kidney Diseases grants: DK104897 to SEK, DK118944 to CML, and DK116558 to ANS. Clozapine-N-Oxide was kindly provided by the National Institute of Mental Health. The authors are grateful to the Kanoski lab undergraduates for their assistance in behavioral experiments and histology.

Figure 1

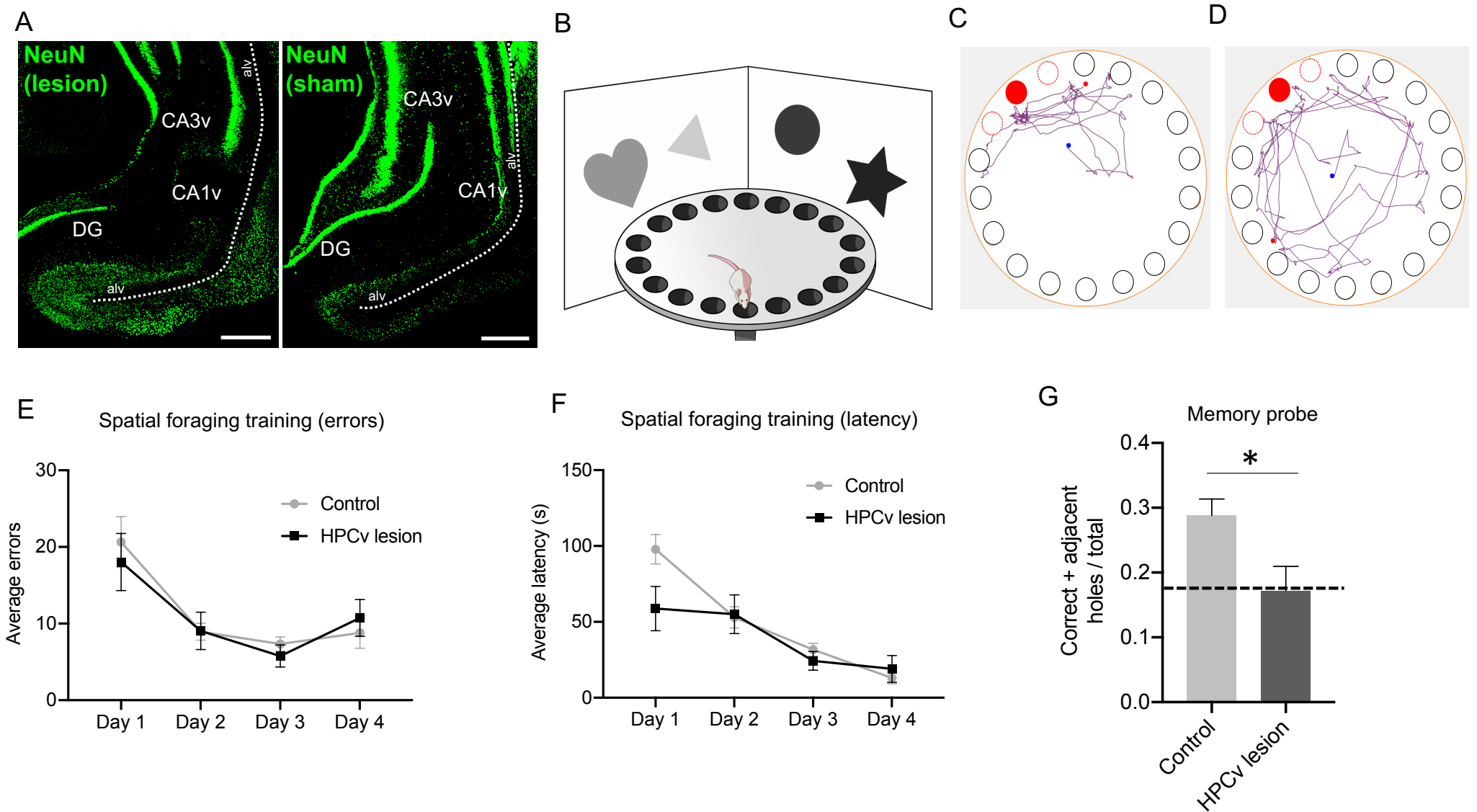
A
NeuN (lesion)
CA3v
CA1v
DG
alv
alv
NeuN (sham)
CA3v
CA1v
DG
alv
alv
B
C
D
E
Spatial foraging training (errors)
Average errors
30
20
10
0
Control
HPCv lesion
Day 1
Day 2
Day 3
Day 4
F
Spatial foraging training (latency)
Average latency (s)
150
100
50
0
Control
HPCv lesion
Day 1
Day 2
Day 3
Day 4
G
Memory probe
Correct + adjacent holes / total
0.4
0.3
0.2
0.1
0.0
*
Control
HPCv lesion

792 **Figure 1. Bilateral HPCv lesions impair spatial memory for food location.** Representative
793 HPCv lesion histology with NeuN immunohistochemistry (A; scale bars 500μm). Spatial
794 foraging task apparatus (B). Representative navigation paths of a control animal preferentially
795 investigating correct (filled red) and adjacent holes (outlined orange) during spatial foraging
796 memory probe (C). Representative navigation path of HPCv lesioned animal during spatial
797 foraging memory probe (D). Bilateral HPCv lesions did not impair learning of the spatial
798 foraging task compared to controls, as measured by errors before locating correct hole during
799 task training (E) and latency to locate correct hole during task training (F). Bilateral HPCv
800 lesions impaired retention of the spatial foraging task, as measured by the ratio of investigation
801 of correct plus adjacent holes over total investigated during the first minute of the task ($p<0.05$;
802 G). There were no group differences observed when evaluated over the entire two minutes of the
803 task (H). Dotted line indicates chance performance level (0.167). For graphs 1D-G, lesion n = 11,
804 control n = 18. All values expressed as mean +/- SEM.
805
806

Figure 2

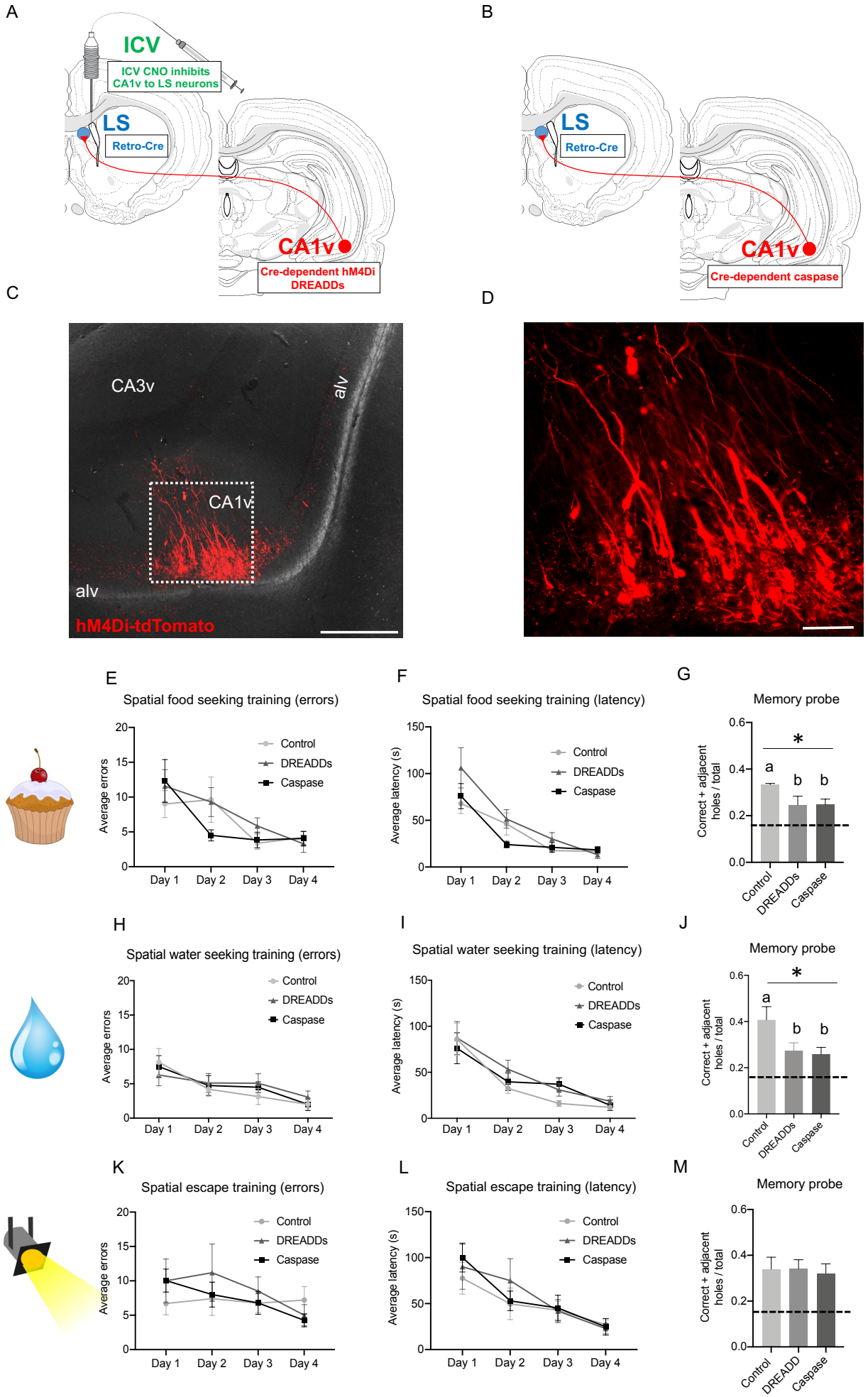
A
ICV
ICV CNO inhibits CA1v to LS neurons
LS
Retro-Cre
CA1v
Cre-dependent hM4Di DREADDs
B
LS
Retro-Cre
CA1v
Cre-dependent caspase
C
CA3v
alv
CA1v
alv
hM4Di-tdTomato
D
E
Spatial food seeking training (errors)
Average errors
Control
DREADDs
Caspase
Day 1
Day 2
Day 3
Day 4
F
Spatial food seeking training (latency)
Average latency (s)
G
Memory probe
Correct + adjacent holes / total
a
b
b
Control
DREADDs
Caspase
H
Spatial water seeking training (errors)
I
Spatial water seeking training (latency)
J
Memory probe
K
Spatial escape training (errors)
L
Spatial escape training (latency)
M
Memory probe
DREADD

807 **Figure 2. Reversible and chronic CA1v to LS neural disconnection impairs spatial memory**
808 **for food and water location but not for escape location.** Diagram of dual viral approach using
809 a cre-dependent inhibitory DREADDs approach to reversibly disconnect CA1v to LS neural
810 pathway (A). Diagram of dual viral approach using a cre-dependent caspase approach to
811 chronically disconnect CA1v to LS neural pathway (B). Representative injection site in CA1v
812 demonstrating LS-projecting neurons infected with inhibitory DREADDs, which simultaneously
813 drives expression of a fluorescent tdTomato transgene (C, D; scale bars 500μm and 100μm,
814 respectively). Neither reversible (DREADDs) nor chronic (caspase) disconnection of the CA1v
815 to LS pathway impaired learning of the spatial food seeking task compared to controls, as
816 measured by errors before correct hole during task training (E) and latency to correct hole during
817 task training (F). Both reversible and chronic disconnection of the CA1v to LS pathway impaired
818 retention of the food location as measured by the ratio of investigation of correct plus adjacent
819 holes over total investigations during entire two minutes of the task ($p<0.05$; G). Likewise,
820 reversible (DREADDs) and chronic (caspase) disconnection of the CA1v to LS pathway did not
821 impair learning of the spatial water seeking task compared to controls, as measured by errors
822 before correct hole during task training (H) and latency to correct hole during task training (I),
823 but impaired memory retention of the water location during the probe (J). In contrast,
824 disconnection of the CA1v to LS pathway either reversibly (DREADDs) or chronically (caspase)
825 did not impair performance on the spatial escape task. There were no differences in learning as
826 measured by errors before correct hole during task training (K) and latency to correct hole during
827 task training (L). Unlike the spatial foraging task, retention of the spatial escape task was not
828 impaired by reversible nor chronic disconnection of the CA1v to LS pathway (M). For graphs
829 2E-G (CA1v to LS disconnect cohort 1), DREADDs n=6, caspase n=10, control n=8. For graphs
830 2H-J (CA1v to LS disconnect cohort 3), DREADDs n=8, caspase n=8, control n=7). For graphs
831 2K-M (CA1v to LS disconnect cohort 2), DREADDs n=8, caspase n=12, control n=10. Dotted
832 line indicates chance performance level (0.167). All values expressed as mean +/- SEM.
833
834

Figure 3

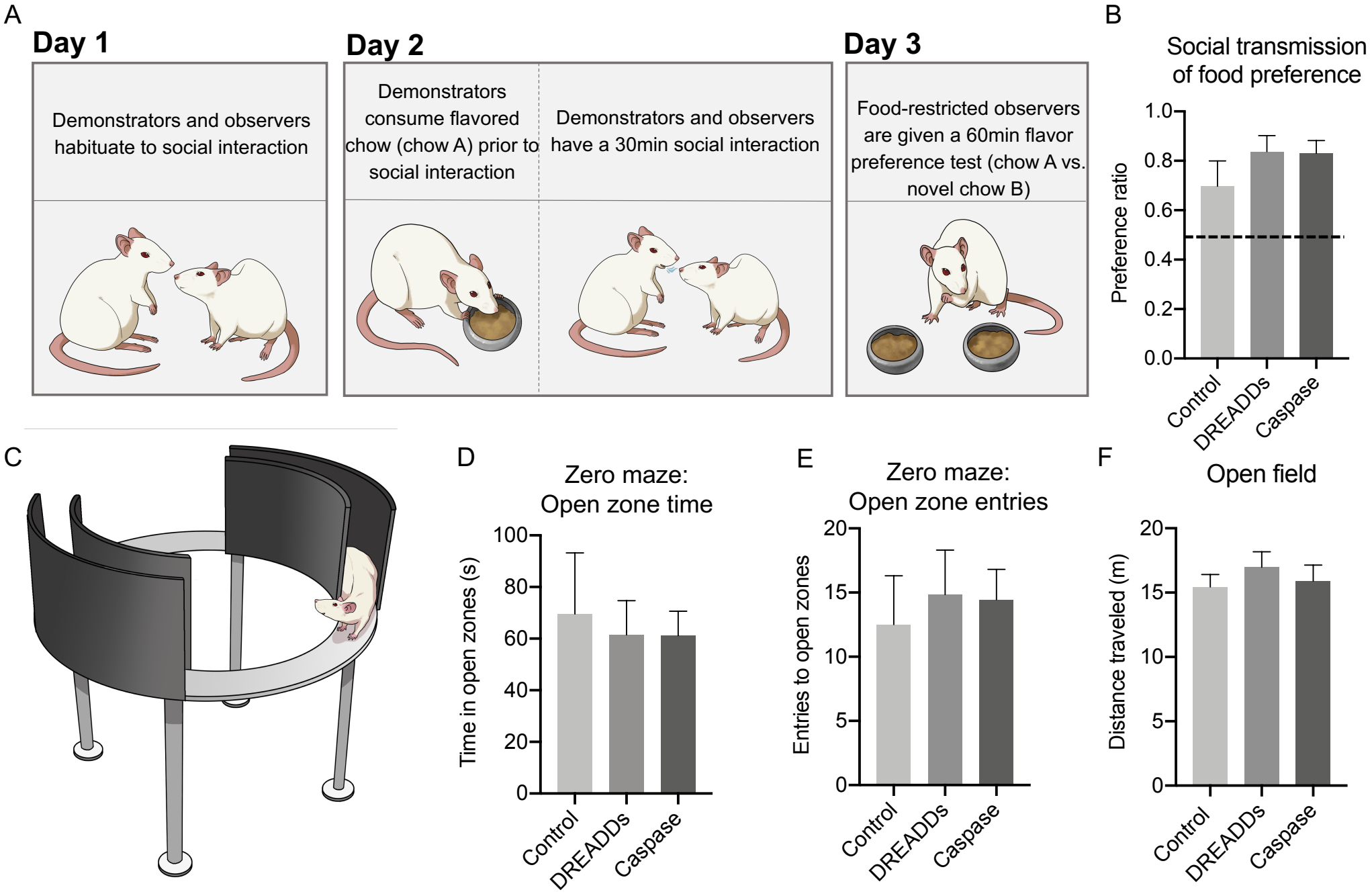
A
Day 1
Demonstrators and observers habituate to social interaction
Day 2
Demonstrators consume flavored chow (chow A) prior to social interaction
Demonstrators and observers have a 30min social interaction
Day 3
Food-restricted observers are given a 60min flavor preference test (chow A vs. novel chow B)
B
Social transmission of food preference
Preference ratio
1.0
0.8
0.6
0.4
0.2
0.0
Control
DREADDs
Caspase
C
D
Zero maze: Open zone time
Time in open zones (s)
100
80
60
40
20
0
Control
DREADDs
Caspase
E
Zero maze: Open zone entries
Entries to open zones
20
15
10
5
0
Control
DREADDs
Caspase
F
Open field
Distance traveled (m)
20
15
10
5
0
Control
DREADDs
Caspase

835 **Figure 3. Neither reversible nor chronic CA1v to LS neural disconnection impair spatial**
836 **memory for escape location, social transmission of food preference, anxiety-like behavior,**
837 **or general locomotor activity levels.** Diagram of the social transmission of food preference
838 (STFP) task (A). Neither reversible nor chronic disconnection of the CA1v to LS pathway impair
839 STFP learning compared to controls, as measured by a food preference ratio (B), with the dotted
840 line indicating chance preference level (0.50). Diagram of the zero maze apparatus (C). Anxiety-
841 like behavior was not influenced by reversible or chronic disconnection of the CA1v to LS
842 pathway compared to controls, as measured by performance in the zero maze task, specifically
843 time in open zones (D) and entries into open zones (E). Neither chronic nor reversible CA1v to
844 LS disconnection affected open field performance compared to controls, as measured by total
845 distance traveled (F). For graphs 3B, 3D, and 3E (CA1v to LS disconnect cohort 1), DREADDs
846 n=6, caspase n=10, control n=8. For graph 3F (CA1v to LS disconnect cohort 2), DREADDs
847 n=8, caspase n=12, control n=10. All values expressed as mean +/- SEM.
848
849

Figure 4

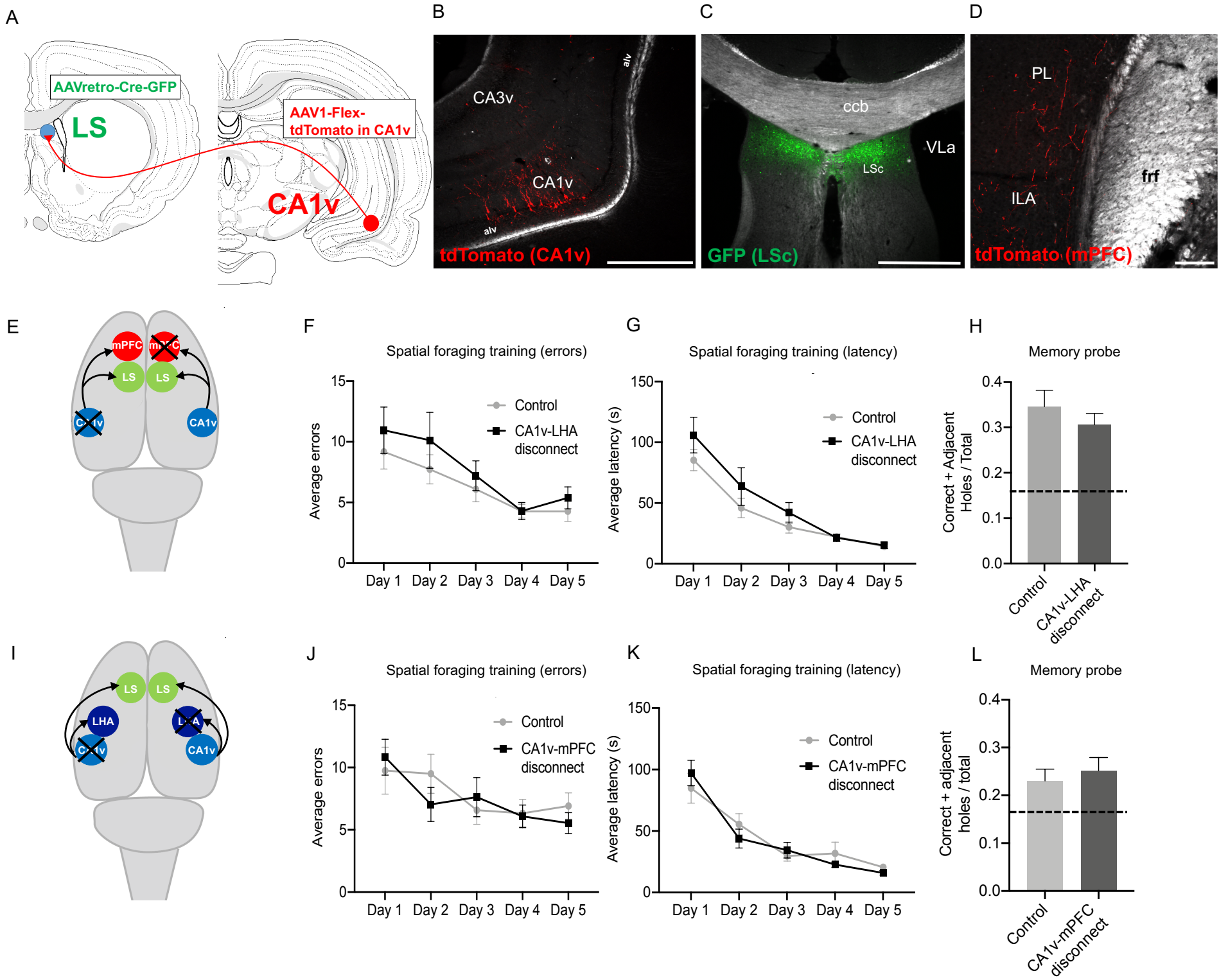
A
AAVretro-Cre-GFP
LS
AAV1-Flex-
tdTomato in CA1v
CA1v
B
CA3v
alv
CA1v
alv
tdTomato (CA1v)
C
ccb
VLa
LSc
GFP (LSc)
D
PL
ILA
frf
tdTomato (mPFC)
E
mPFC
mPFC
LS
LS
CA1v
CA1v
F
Spatial foraging training (errors)
Average errors
Control
CA1v-LHA
disconnect
Day 1
Day 2
Day 3
Day 4
Day 5
G
Spatial foraging training (latency)
Average latency (s)
Control
CA1v-LHA
disconnect
H
Memory probe
Correct + Adjacent
Holes / Total
Control
CA1v-LHA
disconnect
I
LS
LS
LHA
LHA
CA1v
CA1v
J
Spatial foraging training (errors)
Average errors
Control
CA1v-mPFC
disconnect
K
Spatial foraging training (latency)
Average latency (s)
Control
CA1v-mPFC
disconnect
L
Memory probe
Correct + adjacent
holes / total
Control
CA1v-mPFC
disconnect

850 **Figure 4. Neither CA1v to mPFC nor CA1v to LHA disconnection impairs spatial memory**
851 **for food location.** Diagram of dual viral approach to identify collateral targets of the CA1v to
852 LS neural pathway (A). Representative CA1v injection site from collateral identification
853 approach (B; scale bar 500µm). Representative LS injection site from collateral identification
854 approach (C; scale bar 500µm). Representative image collateral axons of the CA1v to LS
855 pathway located in the mPFC (D; scale bar 50µm). Diagram of contralesional approach to
856 functionally disconnect the CA1v to mPFC neural pathway (E). Disconnection of the CA1v to
857 mPFC neural pathway did not influence learning of the spatial foraging task compared to
858 controls, as measured by errors before correct hole during training (F) and latency to correct hole
859 during training (G). Disconnection of the CA1v to mPFC pathway did not influence retention of
860 the spatial foraging task in the memory probe (H). Diagram of contralesional approach to
861 functionally disconnect the CA1v to LHA neural pathway (I). Disconnection of the CA1v to
862 LHA neural pathway did not influence learning of the spatial foraging task compared to controls,
863 as measured by errors before correct hole during training (J) and latency to correct hole during
864 training (K). Disconnection of the CA1v to LHA pathway did not influence retention of the
865 spatial foraging task in the memory probe (L). For graphs 4F-I, CA1v to mPFC disconnect n=12,
866 control n=12. For graphs 4K-N, CA1v to LHA disconnect n=12, control n=11. All values
867 expressed as mean +/- SEM.
868
869

Figure 5

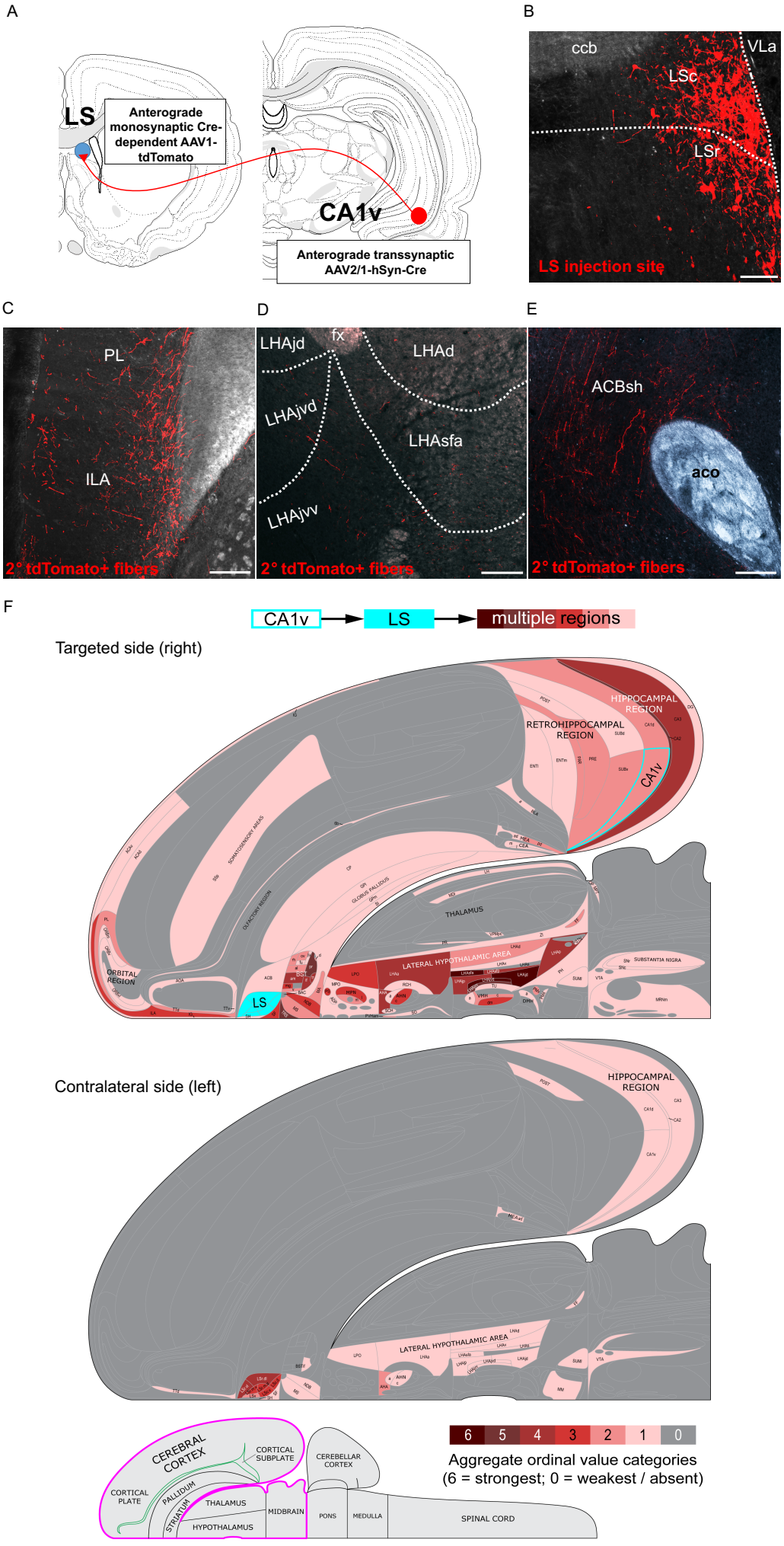
A
LS
Anterograde monosynaptic Cre-dependent AAV1-tdTomato
CA1v
Anterograde transsynaptic AAV2/1-hSyn-Cre
B
ccb
VLa
LSc
LSr
LS injection site
C
PL
ILA
2° tdTomato+ fibers
D
LHAjd
fx
LHAd
LHAjvd
LHAsfa
LHAjvv
2° tdTomato+ fibers
E
ACBsh
aco
2° tdTomato+ fibers
F
CA1v
LS
multiple regions
Targeted side (right)
HIPPOCAMPAL REGION
RETROHIPPOCAMPAL REGION
CA1v
THALAMUS
LATERAL HYPOTHALAMIC AREA
SUBSTANTIA NIGRA
ORBITAL REGION
LS
Contralateral side (left)
HIPPOCAMPAL REGION
LATERAL HYPOTHALAMIC AREA
CEREBRAL CORTEX
CORTICAL SUBPLATE
CORTICAL PLATE
PALLIDUM
STRIATUM
THALAMUS
HYPOTHALAMUS
MIDBRAIN
CEREBELLAR CORTEX
PONS
MEDULLA
SPINAL CORD
6 5 4 3 2 1 0
Aggregate ordinal value categories
(6 = strongest; 0 = weakest / absent)

870 **Figure 5. Identification of second-order neural projections downstream of CA1v to LS**
871 **projections.** Diagram of dual viral approach to identify brain regions that are second-order (2°)
872 targets of the CA1v to LS neural pathway (A). Representative LS injection site from second
873 order identification approach (B; scale bar 100μm). Representative image of second-order fibers
874 of the CA1v to LS pathway within the mPFC (C; scale bar 200μm). Representative image of
875 second-order fibers of the CA1v to LS pathway within the LHA (D; scale bar 200μm).
876 Representative image of second-order fibers of the CA1v to LS pathway within the ACB (E;
877 scale bar 200μm). Summary of the projection targets of LS neurons that receive input from
878 CA1v (F). The outputs of the right side of LS neurons receiving CA1v input are represented at
879 the macroscale (gray matter region resolution) on a partial flatmap representation of the rat
880 forebrain, adapted from (65). Connection weights are represented block colors for each region
881 following an ordinal scale ranging from weakest (0 = very weak or absent) to strongest (6 =
882 strong), as there were no 7 (very strong) values. The inset at lower left represents one side of the
883 brain with the part represented in the upper diagrams outlined in magenta.
884
885

886 **SUPPLEMENTARY INFORMATION**

887

888

Supplemental Figure 1

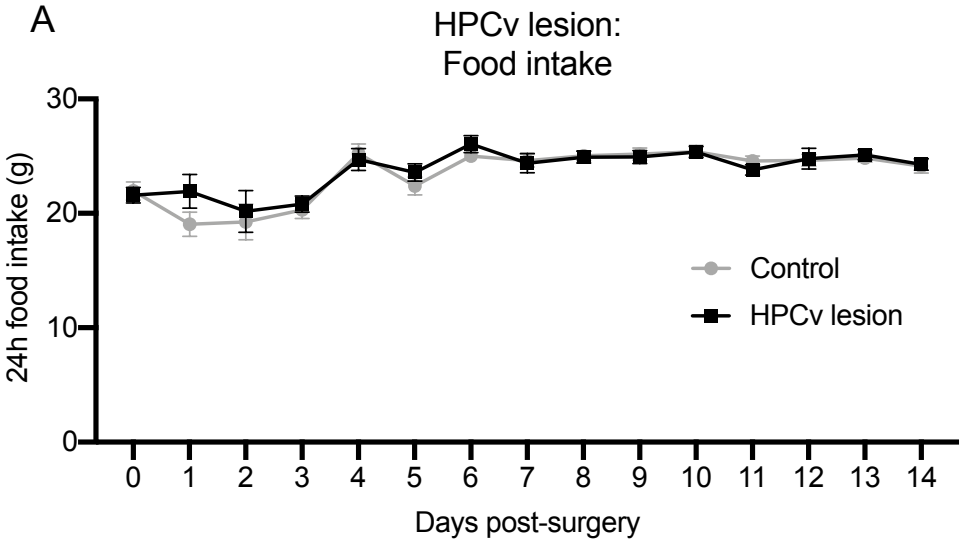

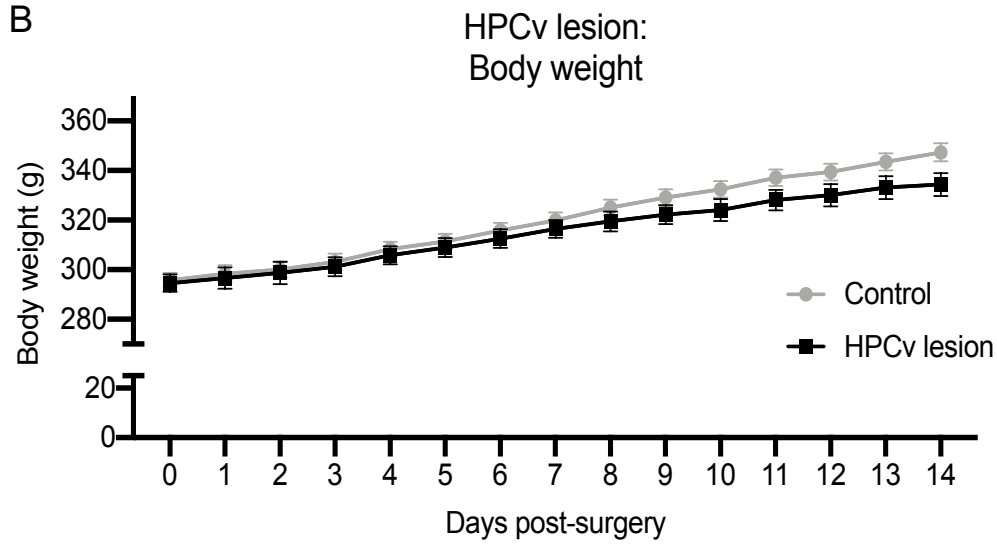

889 **Supplementary Figure 1. Effect of bilateral HPCv lesions on food intake and body weight.**
890 There were no effects on food intake (A) or body weight (B) of bilateral HPCv lesions compared
891 to controls. Lesion n = 11, control n = 18. All values expressed as mean +/- SEM.
892
893

Supplemental Figure 2

A

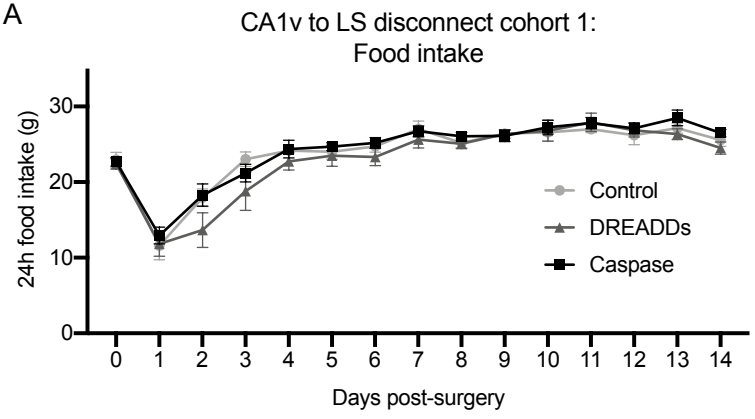

B

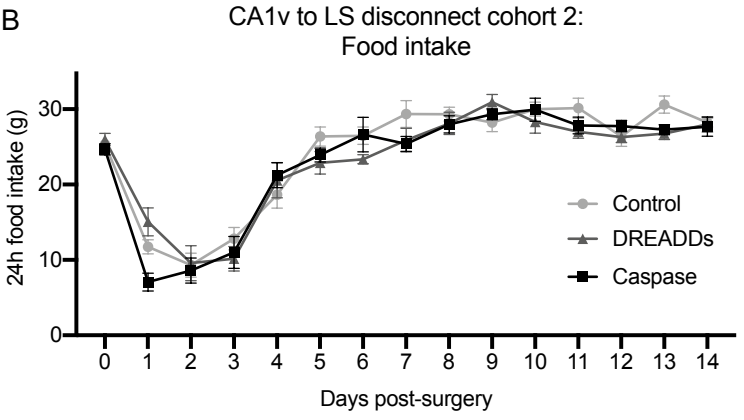

C

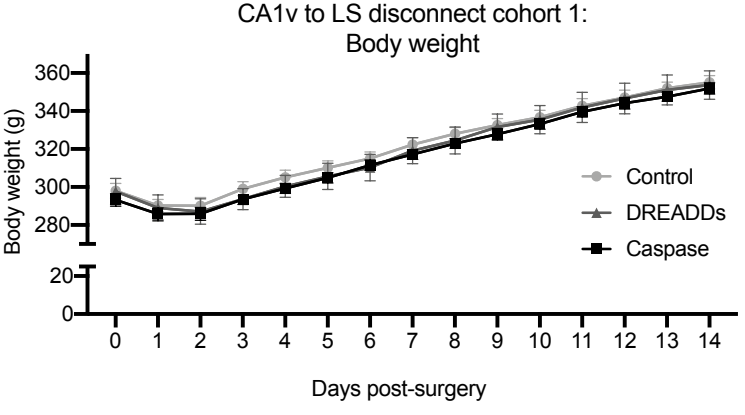

D

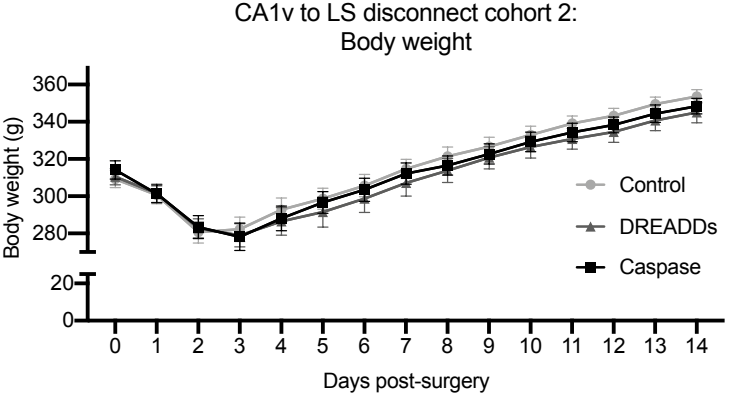

E

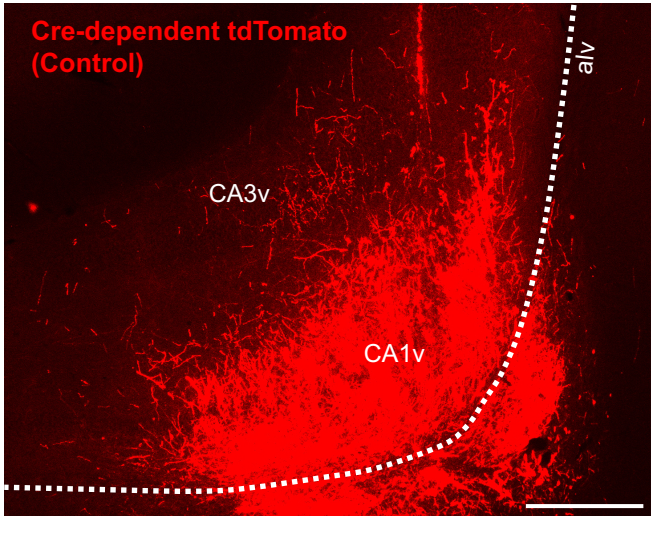

F

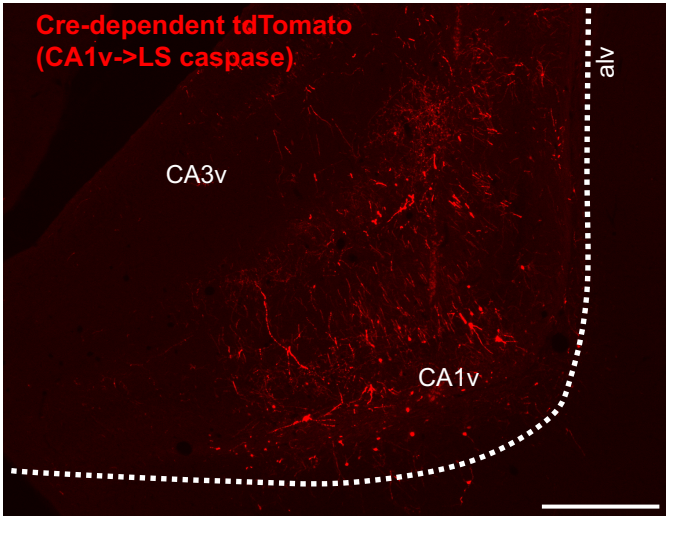

894 **Supplementary Figure 2. Effect of reversible and chronic disconnection of the CA1v to LS**
895 **neural pathway on food intake and body weight, and verification of the chronic approach.**
896 There were no effects on food intake (cohort 1: A; cohort 2: B) or body weight (cohort 1: C;
897 cohort 2: D) of reversible (DREADDs) or chronic (caspase) disconnection of the CA1v to LS
898 neural pathway compared to controls. Histological verification of the dual viral approach
899 demonstrates that cre-dependent tdTomato labeling of CA1v neurons induced by LS-origin retro-
900 cre is robust in a control animal (E), but reduced in an animal injected with cre-dependent
901 caspase combined with cre-dependent tdTomato due to caspase-induced cell death (F). For
902 graphs S1A-B (CA1v to LS disconnect cohort 1), DREADDs n=6, caspase n=10, control n=8.
903 For graphs S1C-D (CA1v to LS disconnect cohort 2), DREADDs n=8, caspase n=12, control
904 n=10. All values expressed as mean +/- SEM.
905

Supplemental Figure 3

Chronic Disconnection of the vCA1-LS Pathway

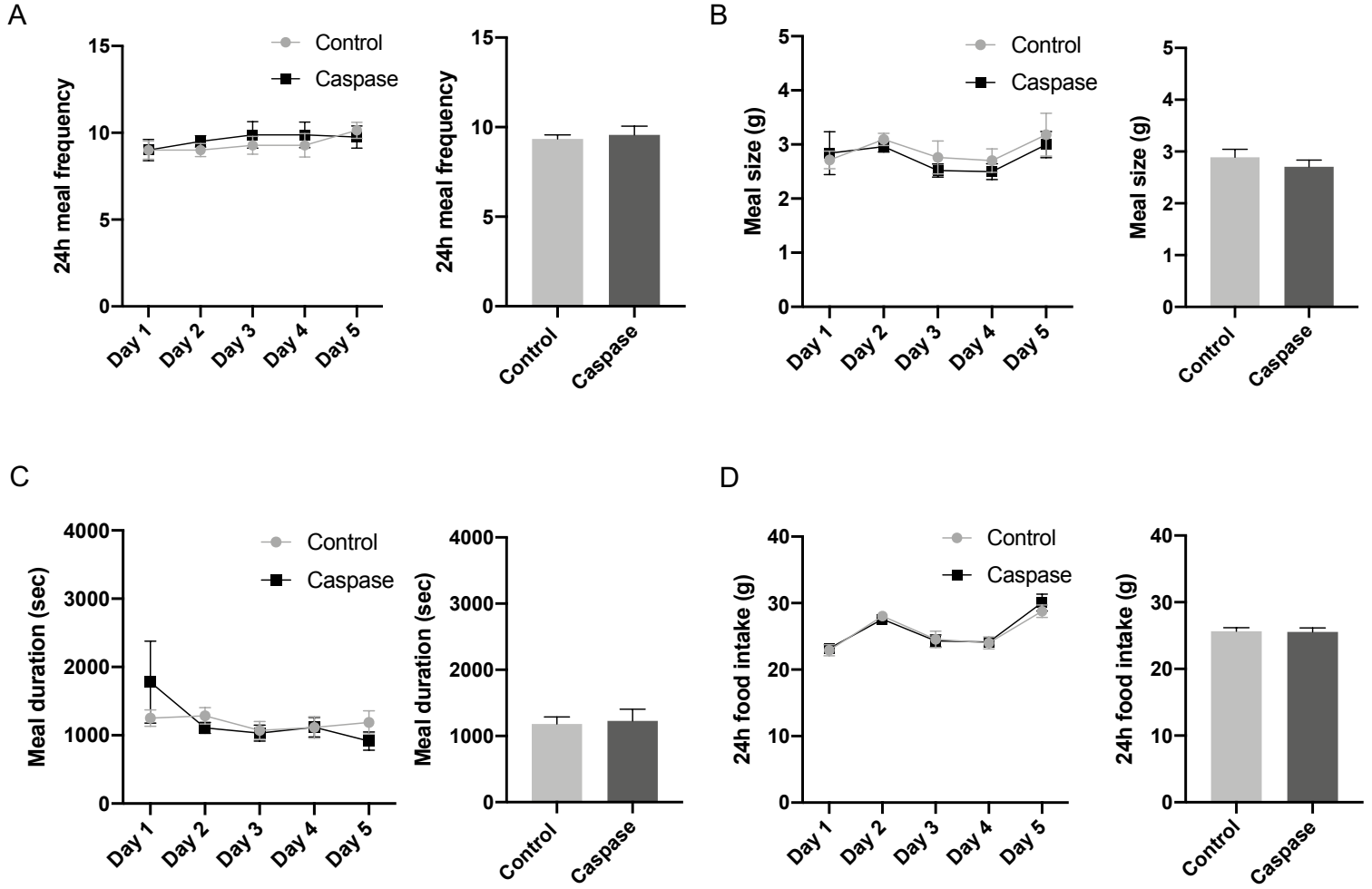

Acute Disconnection of the vCA1-LS Pathway

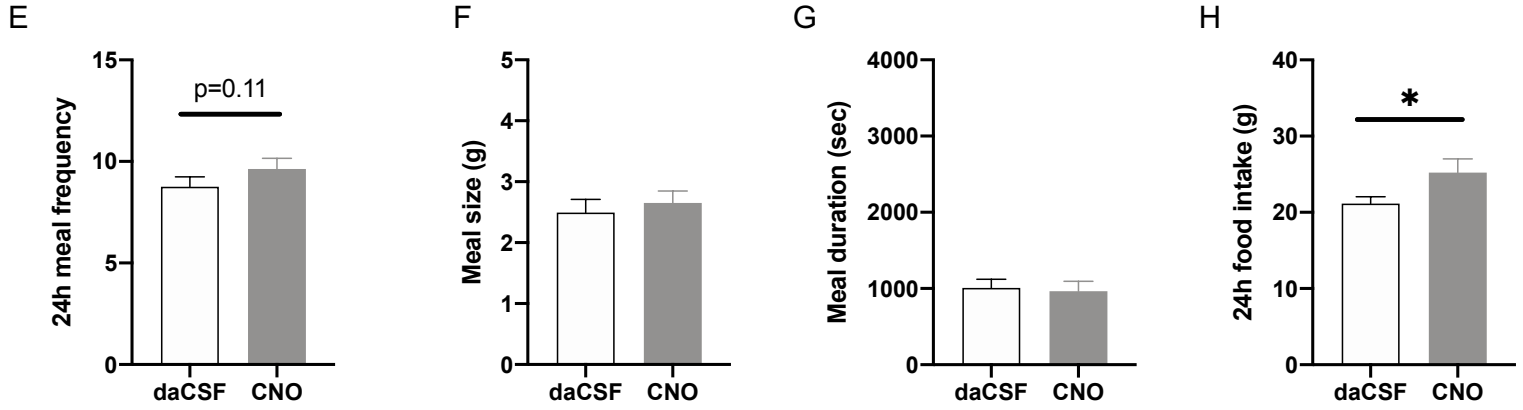

906 **Supplementary Figure 3. Effect of reversible and chronic disconnection of CA1v to LS**
907 **neural pathway on feeding behavior.** Compared with control animals, chronic caspase-
908 mediated disconnection of the CA1v to LS pathway did not significantly affect meal frequency
909 (A), meal size (B), meal duration (C), or 24h cumulative food intake (D) over the course of the
910 5-day recording period. Acute DREADDs-mediated disconnection of the CA1v to LS pathway
911 (via CNO infusion) resulted in non-significant trend towards increased meal frequency (E), no
912 differences in meal size (F) or meal duration (G), and a significant increase in 24h cumulative
913 food intake (H) in comparison with vehicle injection. All values expressed as mean +/- SEM.
914

Supplemental Figure 4

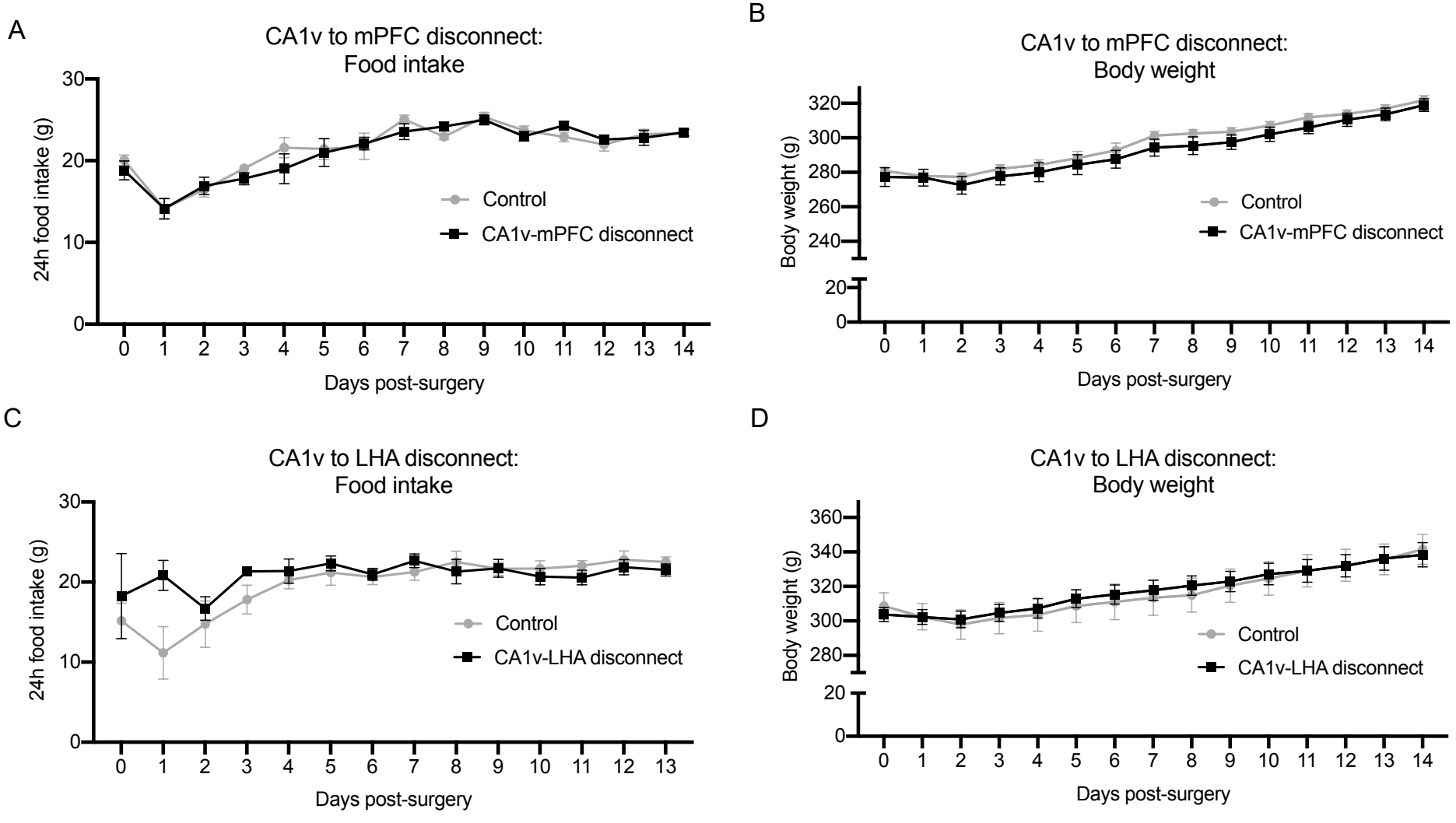

915 **Supplementary Figure 4. Effect of contralesional disconnection methods on food intake and**
916 **body weight.** There were no effects on food intake (A) or body weight (B) of contralesional
917 CA1v to mPFC compared to controls. CA1v to mPFC disconnect n=12, control n=12. There
918 were no effects on food intake (C) or body weight (D) of contralesional CA1v to LHA compared
919 to controls. CA1v to LHA disconnect n=12, control n=11. All values expressed as mean +/-
920 SEM.
921
922

928 **REFERENCES**

929

930 1. R. D'Hooge, P. P. De Deyn, Applications of the Morris water maze in the study of
931 learning and memory. *Brain Res Brain Res Rev* **36**, 60-90 (2001).
932 2. K. Gawel, E. Gibula, M. Marszalek-Grabska, J. Filarowska, J. H. Kotlinska, Assessment of
933 spatial learning and memory in the Barnes maze task in rodents-methodological
934 consideration. *Naunyn Schmiedebergs Arch Pharmacol* **392**, 1-18 (2019).
935 3. R. G. M. Morris, U. Frey, "Hippocampal synaptic plasticity: Role in spatial learning or the
936 automatic recording of attended experience?" in Burgess, Neil (Ed); Jeffery, Kathryn J
937 (Ed); et al (1999) The hippocampal and parietal foundations of spatial cognition. (Oxford
938 University Press, U Edinburgh, Ctr for Neuroscience, Edinburgh, Scotland London, 1999),
939 pp. 220-246.
940 4. D. C. Rowland, Y. Roudi, M. B. Moser, E. I. Moser, Ten Years of Grid Cells. *Annu Rev*
941 *Neurosci* **39**, 19-40 (2016).
942 5. R. Morris, Developments of a water-maze procedure for studying spatial learning in the
943 rat. *Journal of neuroscience methods* **11**, 47-60 (1984).
944 6. C. A. Barnes, Memory deficits associated with senescence: a neurophysiological and
945 behavioral study in the rat. *J Comp Physiol Psychol* **93**, 74-104 (1979).
946 7. J. O'Keefe, J. Dostrovsky, The hippocampus as a spatial map: preliminary evidence from
947 unit activity in the freely-moving rat. *Brain research* (1971).
948 8. T. Hafting, M. Fyhn, S. Molden, M. B. Moser, E. I. Moser, Microstructure of a spatial map
949 in the entorhinal cortex. *Nature* **436**, 801-806 (2005).
950 9. M. S. Fanselow, H.-W. Dong, Are the dorsal and ventral hippocampus functionally
951 distinct structures? *Neuron* **65**, 7-19 (2010).
952 10. A. T. Keinath *et al.*, Precise spatial coding is preserved along the longitudinal
953 hippocampal axis. *Hippocampus* **24**, 1533-1548 (2014).
954 11. K. B. Kjelstrup *et al.*, Finite scale of spatial representation in the hippocampus. *Science*
955 **321**, 140-143 (2008).
956 12. L. de Hoz, J. Knox, R. G. Morris, Longitudinal axis of the hippocampus: both septal and
957 temporal poles of the hippocampus support water maze spatial learning depending on
958 the training protocol. *Hippocampus* **13**, 587-603 (2003).
959 13. J. Ferbinteanu, C. Ray, R. J. McDonald, Both dorsal and ventral hippocampus contribute
960 to spatial learning in Long-Evans rats. *Neurosci Lett* **345**, 131-135 (2003).
961 14. M. B. Moser, E. I. Moser, Functional differentiation in the hippocampus. *Hippocampus* **8**,
962 608-619 (1998).
963 15. S. E. Kanoski, H. J. Grill, Hippocampus Contributions to Food Intake Control: Mnemonic,
964 Neuroanatomical, and Endocrine Mechanisms. *Biol Psychiatry* **81**, 748-756 (2017).
965 16. P. G. Henke, Hippocampal pathway to the amygdala and stress ulcer development. *Brain*
966 *Res Bull* **25**, 691-695 (1990).
967 17. K. G. Kjelstrup *et al.*, Reduced fear expression after lesions of the ventral hippocampus.
968 *Proceedings of the National Academy of Sciences* **99**, 10825-10830 (2002).

969 18. S. Gaskin, A. Gamliel, M. Tardif, E. Cole, D. G. Mumby, Incidental (unreinforced) and
970 reinforced spatial learning in rats with ventral and dorsal lesions of the hippocampus.
971 *Behav Brain Res* **202**, 64-70 (2009).
972 19. M. S. Bienkowski *et al.*, Integration of gene expression and brain-wide connectivity
973 reveals the multiscale organization of mouse hippocampal networks. *Nat Neurosci* **21**,
974 1628-1643 (2018).
975 20. R. Hannapel *et al.*, Postmeal Optogenetic Inhibition of Dorsal or Ventral Hippocampal
976 Pyramidal Neurons Increases Future Intake. *eNeuro* **6** (2019).
977 21. R. C. Hannapel, Y. H. Henderson, R. Nalloor, A. Vazdarjanova, M. B. Parent, Ventral
978 hippocampal neurons inhibit postprandial energy intake. *Hippocampus* **27**, 274-284
979 (2017).
980 22. B. K. Mani *et al.*, Neuroanatomical characterization of a growth hormone secretagogue
981 receptor-green fluorescent protein reporter mouse. *J Comp Neurol* **522**, 3644-3666
982 (2014).
983 23. J. M. Zigman, J. E. Jones, C. E. Lee, C. B. Saper, J. K. Elmquist, Expression of ghrelin
984 receptor mRNA in the rat and the mouse brain. *J Comp Neurol* **494**, 528-548 (2006).
985 24. I. Merchenthaler, M. Lane, P. Shughrue, Distribution of pre-pro-glucagon and glucagon-
986 like peptide-1 receptor messenger RNAs in the rat central nervous system. *J Comp*
987 *Neurol* **403**, 261-280 (1999).
988 25. S. E. Kanoski, S. M. Fortin, K. M. Ricks, H. J. Grill, Ghrelin signaling in the ventral
989 hippocampus stimulates learned and motivational aspects of feeding via PI3K-Akt
990 signaling. *Biol Psychiatry* **73**, 915-923 (2013).
991 26. S. E. Kanoski *et al.*, Hippocampal leptin signaling reduces food intake and modulates
992 food-related memory processing. *Neuropsychopharmacology* **36**, 1859-1870 (2011).
993 27. T. M. Hsu *et al.*, A hippocampus to prefrontal cortex neural pathway inhibits food
994 motivation through glucagon-like peptide-1 signaling. *Mol Psychiatry* **23**, 1555-1565
995 (2018).
996 28. T. M. Hsu, J. D. Hahn, V. R. Konanur, A. Lam, S. E. Kanoski, Hippocampal GLP-1 receptors
997 influence food intake, meal size, and effort-based responding for food through volume
998 transmission. *Neuropsychopharmacology* **40**, 327-337 (2015).
999 29. A. N. Suarez, C. M. Liu, A. M. Cortella, E. E. Noble, S. E. Kanoski, Ghrelin and Orexin
1000 Interact to Increase Meal Size Through a Descending Hippocampus to Hindbrain
1001 Signaling Pathway. *Biol Psychiatry* **87**, 1001-1011 (2020).
1002 30. G. D. Petrovich, N. S. Canteras, L. W. Swanson, Combinatorial amygdalar inputs to
1003 hippocampal domains and hypothalamic behavior systems. *Brain research reviews* **38**,
1004 247-289 (2001).
1005 31. C. De La Rosa-Prieto *et al.*, Subicular and CA1 hippocampal projections to the accessory
1006 olfactory bulb. *Hippocampus* **19**, 124-129 (2009).
1007 32. T. M. Hsu *et al.*, Hippocampus ghrelin receptor signaling promotes socially-mediated
1008 learned food preference. *Neuropharmacology* **131**, 487-496 (2018).
1009 33. L. W. Swanson, W. M. Cowan, An autoradiographic study of the organization of the
1010 efferent connections of the hippocampal formation in the rat. *J Comp Neurol* **172**, 49-84
1011 (1977).

1012 34. T. M. Hsu *et al.*, Hippocampus ghrelin signaling mediates appetite through lateral
1013 hypothalamic orexin pathways. *Elife* **4** (2015).
1014 35. A. Arszovszki, Z. Borhegyi, T. Klausberger, Three axonal projection routes of individual
1015 pyramidal cells in the ventral CA1 hippocampus. *Front Neuroanat* **8**, 53 (2014).
1016 36. P. Y. Risold, L. W. Swanson, Structural evidence for functional domains in the rat
1017 hippocampus. *Science (New York, N.Y.)* **272**, 1484-1486 (1996).
1018 37. P. Sweeney, Y. Yang, An excitatory ventral hippocampus to lateral septum circuit that
1019 suppresses feeding. *Nat Commun* **6**, 10188 (2015).
1020 38. R. Garcia, R. M. Vouimba, R. Jaffard, Spatial discrimination learning induces LTP-like
1021 changes in the lateral septum of mice. *Neuroreport: An International Journal for the*
1022 *Rapid Communication of Research in Neuroscience* **5**, 329-332 (1993).
1023 39. R. Jaffard, R. M. Vouimba, A. Marighetto, R. Garcia, Long-term potentiation and long-
1024 term depression in the lateral septum in spatial working and reference memory. *J*
1025 *Physiol Paris* **90**, 339-341 (1996).
1026 40. S. J. Terrill *et al.*, Nucleus accumbens melanin-concentrating hormone signaling
1027 promotes feeding in a sex-specific manner. *Neuropharmacology* **178**, 108270 (2020).
1028 41. A. Carballo-Marquez, A. Vale-Martinez, G. Guillazo-Blanch, M. Marti-Nicolovius,
1029 Muscarinic receptor blockade in ventral hippocampus and prelimbic cortex impairs
1030 memory for socially transmitted food preference. *Hippocampus* **19**, 446-455 (2009).
1031 42. R. A. Countryman, N. L. Kaban, P. J. Colombo, Hippocampal c-fos is necessary for long-
1032 term memory of a socially transmitted food preference. *Neurobiol Learn Mem* **84**, 175-
1033 183 (2005).
1034 43. G. M. Parfitt *et al.*, Bidirectional Control of Anxiety-Related Behaviors in Mice: Role of
1035 Inputs Arising from the Ventral Hippocampus to the Lateral Septum and Medial
1036 Prefrontal Cortex. *Neuropsychopharmacology : official publication of the American*
1037 *College of Neuropsychopharmacology* **42**, 1715-1728 (2017).
1038 44. N. L. Trent, J. L. Menard, The ventral hippocampus and the lateral septum work in
1039 tandem to regulate rats' open-arm exploration in the elevated plus-maze. *Physiology &*
1040 *behavior* **101**, 141-152 (2010).
1041 45. J. C. Jimenez *et al.*, Anxiety Cells in a Hippocampal-Hypothalamic Circuit. *Neuron* **97**,
1042 670-683.e676 (2018).
1043 46. M. S. Fanselow, H. W. Dong, Are the dorsal and ventral hippocampus functionally
1044 distinct structures? *Neuron* **65**, 7-19 (2010).
1045 47. M. Contreras, T. Pelc, M. Llofriu, A. Weitzenfeld, J. M. Fellous, The ventral hippocampus
1046 is involved in multi-goal obstacle-rich spatial navigation. *Hippocampus* **28**, 853-866
1047 (2018).
1048 48. S. L. T. Lee, D. Lew, V. Wickenheisser, E. J. Markus, Interdependence between dorsal and
1049 ventral hippocampus during spatial navigation. *Brain Behav* **9**, e01410 (2019).
1050 49. D. P. Holschneider *et al.*, Cerebral perfusion mapping during retrieval of spatial memory
1051 in rats. *Behavioural brain research* **375**, 112116 (2019).
1052 50. D. Olivo, M. Caba, F. Gonzalez-Lima, J. F. Rodríguez-Landa, A. A. Corona-Morales,
1053 Metabolic activation of amygdala, lateral septum and accumbens circuits during food
1054 anticipatory behavior. *Behav Brain Res* **316**, 261-270 (2017).

1055 51. M. Carus-Cadavieco *et al.*, Gamma oscillations organize top-down signalling to
1056 hypothalamus and enable food seeking. *Nature* **542**, 232-236 (2017).
1057 52. S. J. Terrill *et al.*, Role of lateral septum glucagon-like peptide 1 receptors in food intake.
1058 *American journal of physiology. Regulatory, integrative and comparative physiology* **311**,
1059 R124-132 (2016).
1060 53. S. J. Terrill, K. D. Wall, N. D. Medina, C. B. Maske, D. L. Williams, Lateral septum growth
1061 hormone secretagogue receptor affects food intake and motivation for sucrose
1062 reinforcement. *American journal of physiology. Regulatory, integrative and comparative*
1063 *physiology* **315**, R76-r83 (2018).
1064 54. C. Wang, C. M. Kotz, Urocortin in the lateral septal area modulates feeding induced by
1065 orexin A in the lateral hypothalamus. *American journal of physiology. Regulatory,*
1066 *integrative and comparative physiology* **283**, R358-367 (2002).
1067 55. J. Hauser, L. H. Llano López, J. Feldon, P. A. Gargiulo, B. K. Yee, Small lesions of the dorsal
1068 or ventral hippocampus subregions are associated with distinct impairments in working
1069 memory and reference memory retrieval, and combining them attenuates the
1070 acquisition rate of spatial reference memory. *Hippocampus* **30**, 938-957 (2020).
1071 56. D. S. Olton, The radial arm maze as a tool in behavioral pharmacology. *Physiology &*
1072 *behavior* **40**, 793-797 (1987).
1073 57. H. H. Pothuizen, W. N. Zhang, A. L. Jongen-Rêlo, J. Feldon, B. K. Yee, Dissociation of
1074 function between the dorsal and the ventral hippocampus in spatial learning abilities of
1075 the rat: a within-subject, within-task comparison of reference and working spatial
1076 memory. *The European journal of neuroscience* **19**, 705-712 (2004).
1077 58. L. E. Jarrard, L. P. Luu, T. L. Davidson, A study of hippocampal structure-function
1078 relations along the septo-temporal axis. *Hippocampus* **22**, 680-692 (2012).
1079 59. L. W. Swanson, Brain maps 4.0-Structure of the rat brain: An open access atlas with
1080 global nervous system nomenclature ontology and flatmaps. *J Comp Neurol* **526**, 935-
1081 943 (2018).
1082 60. R. C. Ritter, P. G. Slusser, S. Stone, Glucoreceptors controlling feeding and blood glucose:
1083 location in the hindbrain. *Science* **213**, 451-452 (1981).
1084 61. E. E. Noble *et al.*, Hypothalamus-hippocampus circuitry regulates impulsivity via
1085 melanin-concentrating hormone. *Nat Commun* **10**, 4923 (2019).
1086 62. B. Zingg *et al.*, AAV-Mediated Anterograde Transsynaptic Tagging: Mapping
1087 Corticocollicular Input-Defined Neural Pathways for Defense Behaviors. *Neuron* **93**, 33-
1088 47 (2017).
1089 63. A. N. Suarez *et al.*, Gut vagal sensory signaling regulates hippocampus function through
1090 multi-order pathways. *Nat Commun* **9**, 2181 (2018).
1091 64. J. D. Hahn, O. Sporns, A. G. Watts, L. W. Swanson, Macroscale intrinsic network
1092 architecture of the hypothalamus. *Proc Natl Acad Sci U S A* **116**, 8018-8027 (2019).
1093 65. J. D. Hahn, Swanson, L. W,. Bowman, I., Foster, N. N., Zingg, B., Bienkowski, M. S.,
1094 Hintiryan, H., & Dong, H.-W. , An open access mouse brain flatmap and upgraded rat
1095 and human brain flatmaps based on current reference atlases. *J. Comp. Neurol.* (2020).
1096 66. L. E. Herzog *et al.*, Interaction of Taste and Place Coding in the Hippocampus. *The*
1097 *Journal of neuroscience : the official journal of the Society for Neuroscience* **39**, 3057-
1098 3069 (2019).

1099 67. R. A. Countryman, P. E. Gold, Rapid forgetting of social transmission of food preferences
1100 in aged rats: relationship to hippocampal CREB activation. *Learn Mem* **14**, 350-358
1101 (2007).
1102 68. B. G. Galef, Jr., W. Y. Lee, E. E. Whiskin, Lack of interference in long-term memory for
1103 socially learned food preferences in rats (Rattus norvegicus). *J Comp Psychol* **119**, 131-
1104 135 (2005).
1105 69. B. G. Galef, Jr., E. E. Whiskin, Socially transmitted food preferences can be used to study
1106 long-term memory in rats. *Learn Behav* **31**, 160-164 (2003).
1107